THESIS

SHIFTING SANDS: DRIVERS AND MOBILIZATION OF FINE SEDIMENT ON THE CACHE LA POUDRE RIVER FOLLOWING A WILDFIRE

Submitted by

Aaron C. Katz

Department of Geosciences

In partial fulfillment of the requirements

For the Degree of Master of Science

Colorado State University

Fort Collins, Colorado

Summer 2024

Master's Committee:

Advisor: Ellen Wohl

Kevin Bestgen
Dan McGrath

Copyright by Aaron Katz 2024

All Rights Reserved

ABSTRACT

SHIFTING SANDS: DRIVERS AND MOBILIZATION OF FINE SEDIMENT ON THE CACHE LA POUDRE RIVER FOLLOWING A WILDFIRE

The Cameron Peak wildfire (840 km^2) of 2020 led to widespread but varied detrimental effects throughout the Poudre River watershed (4,895 km^2). The Poudre River flows through a high gradient canyon section with a somewhat unimpaired flow regime before it reaches a low gradient transition zone with several human impacts including channel modifications and flow reduction. Burned tributaries contributed elevated levels of fine sediment (< 2 mm) to the mainstem Poudre within the canyon, and in 2021 a large debris flow in Black Hollow Creek, a canyon tributary, delivered substantial amounts of material, including fine sediment, directly into the mainstem Poudre River. This led to a major fish kill and the transportation and deposition of fine sediment for at least 100 km downstream. In the transition zone, extensive fine sediment deposits either partially blocked or filled several channel margin backwaters and side channels, which are important habitats for native fish, and fine sediment filled interstices of coarse substrate grains in the mainstem river, which impacts benthic macroinvertebrate and fish spawning habitat.

I quantify the degree of fine sediment retention along 100 km of the Poudre River by measuring reach-averaged fine sediment volumes and embeddedness and use model selection of multiple linear regression models to determine whether distance downstream from the sediment source or reach-scale geometric variables are the primary drivers of fine sediment retention. I also conduct a flushing flows study using 2-dimensional hydraulic modelling to determine the discharge required to mobilize the

substrate at four sites along the longitudinal gradient of the study area representing different geomorphic settings and hydrologic regimes.

Results from model selection using Akaike's Information Criterion corrected for small sample size (AIC_c) show that for both metrics of fine sediment retention, reach location (canyon vs. transition zone) is the primary driver of sediment retention, but some reach-scale variables are significant predictors of fine sediment retention. Both fine sediment retention metrics (site-averaged volumes and embeddedness) are greater in the transition zone. At the reach scale, gradient and cross-sectional area are both significant predictors of embeddedness, and models with gradient as a predictor variable have substantial support in explaining site-averaged fine sediment volumes. A mixed model of embeddedness at the transect level with bedform as the fixed effect nested with site as the random effect indicates that fine sediment is preferentially retained in pools and that all backwaters are 100% embedded. Although there are only three sites upstream of Black Hollow, fine sediment retention is either greater or not statistically different than canyon sites downstream of Black Hollow.

Hydraulic modelling of the 2-, 5-, and 10-year recurrence interval flows at four sites indicates major differences in the magnitude and frequency of bed substrate mobilization between the canyon and transition zone. At a high gradient canyon site, the 2-year flow mobilizes a substantial portion of the bed, while at transition zone sites, bed mobilization occurs only at the 5- or 10-year flow level. I posit that artificially reduced flows in the transition zone are responsible for the lack of bed mobilization and will lead to longer residence times of fine sediment and prolonged impacts to aquatic ecosystems.

This study adds to the literature by investigating post-fire fluvial responses at a greater spatial scale than most previous studies of the matter. By quantifying spatial distribution, physical drivers, and mobilization potential of fine sediment following a large wildfire on a major river, we can better

understand how large rivers with varied human impacts respond to major disturbances and make informed management and restoration decisions going forward.

ACKNOWLEDGEMENTS

I would like to extend my gratitude to many people and organizations who supported and guided me through this research. First, I am indebted beyond words to my advisor, Dr. Ellen Wohl, whose guidance and expertise have made me into the fluvial geomorphologist I am today. I thank my committee members Dr. Kevin Bestgen and Dr. Dan McGrath for helping plan, execute, and edit the research. Kevin was instrumental in guiding this study to be applicable to ongoing fisheries research in the wake of the fish kill, and Dan's help with the RTK and drone survey processing was vital. Matthew Haworth helped design this study by selecting transition zone sites, familiarizing me with them, and offering his time to field work. I had so much help in the field in the summer and fall of 2023 starting with my intern, Carl Cruz, who took everything in stride. Thanks to Shayla Triantafillou, Billy Stansfield, and Brady Jones for helping in the field. I had incredible help from the CSU Larval Fish Laboratory crew with transect surveys. Jed Perkins, Trent Moore, Rose Stahl, and Ben Applegate adapted quickly to the data collection procedure and endured some unfavorable conditions on the river. I also thank Christopher Robertson from the CSU Drone Center for guidance and access to the drone used in this study.

Back in the lab, I had help with processing RTK data from Dr. Dan McGrath, Randell Bonnel, and Connor Mertz. I thank Nick Christensen for his HEC-RAS wizardry. Dr. Ann Hess from the CSU Statistics Consulting Lab helped me decide which statistical analyses to use. I also thank the many developers who donate their time to create free, open-source software that is critical for the advancement of scientific understanding, like QGIS, R, and CloudCompare.

I appreciate the CSU Geosciences graduate community for creating a fun and supportive atmosphere that keeps us motivated amidst the stress of graduate school. I thank everyone in the Fluvial Geomorphology lab group for providing amazing mentorship and laughs throughout my time

here. I am grateful for the amazing support from family and friends – my parents, Abby Shifriss, musical collaborators, and many friends near and far keep inspiring me in so many ways. Finally, I would like to send a special thank you to Sara Rathburn and Jim Finley, who fostered the sweetest puppy in the world during the spring of 2023 who I was able to adopt. Thank you for helping me find my best friend, Jack!

TABLE OF CONTENTS

LIST OF TABLES

LIST OF FIGURES

1. INTRODUCTION

As wildfires occur at higher rates and intensities in the western US (United States), they pose increased risks to ecosystems and human infrastructure (Dennison et al., 2014). Wildfires in forested areas initiate a series of altered hydrologic responses starting with increased hillslope runoff and erosion in the burned area (Benavides-Solorio & MacDonald, 2001; Moody & Martin, 2001). Channels downstream of burned areas typically experience increased streamflow (Kunze & Stednick, 2006; Lane et al., 2006), sediment load (Reneau et al., 2007; Ryan et al., 2011), and changes to water chemistry (Minshall et al., 1997), but these responses can vary greatly depending on fire extent and intensity, watershed characteristics, and precipitation after the fire. Changes in fluxes of water, sediment, and ash can impact aquatic habitat (Gresswell, 1999), water quality (Smith et al., 2011), and water supply infrastructure (Writer et al., 2014).

Beyond the first-order effects of wildfires, such as loss of vegetation and burnt soil, second-order effects of increased fluxes of flow and sediment lead to third-order effects on aquatic ecosystems and organisms in receiving waters. Gresswell (1999) found that altered hydrology is likely the primary influence on aquatic ecosystems after fire. Starting at the base of the aquatic food chain, wildfire-related floods and altered sediment loads can reduce macroinvertebrate populations and alter macroinvertebrate composition, but the degree of effects varies based on fire severity and proximity to the fire (Minshall, 2003). As fine sediment fills the interstices of a gravel bed stream, it reduces macroinvertebrate habitat and impedes the ability of fish to work spawning gravels into redds (Kemp et al., 2011). Increased presence of fine sediment, regardless of source, also impacts fish physiology and performance, and it may reduce reproductive success (Kemp et al., 2011).

Understanding wildfires' downstream impacts to fluvial systems is crucial for restoring rivers and aquatic ecosystems and can aid land managers in preparing watersheds for future fires and disturbances. Wildfires typically harm downstream aquatic ecosystems because the wide range of post-

fire fluxes are usually out of balance with baseline levels (summarized in Florsheim & Chin, 2022). A river's response to post-fire fluxes can indicate its resiliency, which has been defined as a system's capacity to absorb disturbance and reorganize itself while continuing to function as before (Walker et al., 2004). In fluvial geomorphology, resilience can be equated to resistance to change, or the ability to recover from disturbances (Reid & Brierley, 2015). Geomorphic complexity is commonly correlated with biodiversity, influences attenuation of downstream fluxes, and is closely connected to resistance and resilience to disturbances (Wohl, 2016). Alterations that reduce geomorphic complexity, such as altered flow regimes, floodplain disconnection, and channelization, reduce a river's resilience and ability to respond to the wide ranges of wildfire-induced fluxes.

This study is concerned with fine sediment deposition and retention on the Cache la Poudre (Poudre) River in the northern Front Range of Colorado, USA after the Cameron Peak wildfire of 2020. A combination of increased sediment supply and a debris flow that delivered large amounts of sediment to the mainstem Poudre River led to a massive fish kill and widespread deposition of fine sediment (pebble-size and finer). Along with tracking the recovery of fish populations and aquatic ecosystem health, it is critical to understand what geomorphic conditions facilitate fine sediment deposition and retention, and what flows are necessary to flush excess fine sediment downstream. Related studies undertaken by fish ecologists will determine the relationship between degree of impact caused directly by the debris flow and subsequent sediment deposition and retention, and fish population and habitat recovery.

1.1 Study Objectives

1.1.1 Fine sediment retention

The first objective of this study is to determine what geomorphic conditions facilitate fine sediment (< 2 mm) retention on the Poudre River. Through field data collection and statistical analyses, I

evaluate whether reach-scale geomorphic attributes or distance downstream from the sediment source is a better predictor of fine sediment retention. Sediment retention is quantified by volumetric surveys of measurable fine sediment deposits and by substrate embeddedness surveys. Field surveys collect reach-scale geomorphic attributes including reach-scale channel gradient, bankfull channel dimensions, channel cross-sectional geometry, bank length ratio, streambed grain-size, and other attributes at each site. Distance downstream along the river is determined via geographic information system (GIS) methods.

This study compares spatial trends in sediment retention and does not account for changes in sediment deposition through time since the wildfire. Although it is not always possible to determine the exact source of a given fine sediment deposit, surveying all deposits suspected of being fire-derived can illuminate the drivers of sediment retention.

1.1.2 Fine sediment mobilization and flushing

The second objective is to use two-dimensional hydraulic modelling and simple incipient motion equations to determine the discharge required to remobilize and remove excess fine sediment by mobilizing the coarse substrate. Four sites were chosen for modelling that represent the range of geomorphic settings and flow regimes throughout the study area. I compare the extent of mobilization at each site for the 2-, 5-, and 10-year flood recurrence interval to evaluate bed mobilization potential.

Flushing flows are undertaken to meet a wide range of objectives ranging from removing fines covering spawning gravels, to mobilizing the coarse armor layer, to channel-forming flow that causes major geomorphic change (Kondolf & Wilcock, 1996). In this study, I use the movement of the coarse armor layer as a flushing flow that will also mobilize embedded fines in the interstitial space. Using the median diameter grain size from each site and established sediment mobilization equations, I determine

a critical shear stress for bed mobilization. Finally, in HEC-RAS 2D, I identify the spatial extent of bed mobilization for a given flood at each site.

1.1.3 Limitations

The timing, scope, and depth of this study naturally lead to certain limitations regarding research findings. First, this study can only make inferences about fine sediment transport and deposition through time because data were collected at a single point in time (one season). The fire occurred in late 2020 and data for this study were collected in summer and fall 2023. Additionally, there are no pre-fire quantitative data to compare my data to. Therefore, temporal trends of fine sediment retention cannot be determined quantitatively, but they can be inferred, while spatial trends can be quantified. This study does not include any measurements of sediment transport via suspended sediment or bed load sampling, so I cannot make any judgements about sediment transport rate. Hydraulic modelling of bed mobilization can illuminate potential for flushing fines from the substrate, but it does not yield information about transport rate or volume.

Study sites are meant to represent the full length of the mainstem Poudre River in the study area, but they are not systematically distributed by distance downstream (i.e., spaced at a fixed distance downstream). Sites were chosen from preexisting fish monitoring sites, so findings from this study can be compared with fish population surveys. Therefore, they may not sample the full range of geomorphic conditions throughout the study area.

Other limitations arise from the many steps taken from field data collection to quantitative metrics, the limited sample size used in statistical models, and other generalizations like bankfull delineation and incipient motion criteria. These are discussed in detail in Section 3 (Methods).

1.2 Background

1.2.1 Fluvial response to wildfires

Fluvial response to wildfires is well documented and includes a wide range of altered processes in the vicinity of the fire and in downstream waterways. The degree of impact is commonly nonlinear in time or space; altered fluxes are more likely to occur in the first few years post-fire and nearest the fire. There is commonly a window of disturbance with increased impacts followed by a gradual return to base level rates, but this timing can vary greatly.

In a review of post-fire responses of hydrology, sediment transport, water quality, and ecological metrics, Paul et al. (2022) found that the median response time of alterations was less than 5 years. For example, increased hillslope erosion rates following the 1996 Buffalo Creek Fire in the Colorado Front Range persisted for three years (Moody & Martin, 2001), and after the 2012 High Park Fire, which burned in the Poudre River watershed, Brogan et al. (2019) found sediment accumulation in wide and flat valley bottoms for 2 years post-fire followed by minor changes 2 years after that in a 15-km^2 watershed. After the 2000 Cerro Grande fire in New Mexico, USA, suspended sediment spiked in the following year and remained significantly above pre-fire averages for five years, while coarse-grained bedload also increased but was associated with snowmelt runoff (Reneau et al., 2007). In a study of post-fire sediment response in Wyoming, Ryan & Dixon (2008) found substantial increases in suspended sediment transport, with highest rates in the first year and a return to baseline levels within a few years, and they found no detectable increases in bedload transport rate. Regarding aquatic ecosystem response, Minshall (2003) found that impacts to benthic macroinvertebrates are restricted to the first 5 to 10 years post-fire and are associated with more intense burns. These examples demonstrate the temporal variation in ecosystem response post-fire.

Wildfires usually occur in headwaters, and therefore post-fire studies are generally conducted in lower-order streams. Studies usually range in size from individual plot scale for tests of post-fire soil treatments (e.g., Díaz-Raviña et al., 2012) to higher-order streams with drainage areas in the tens (e.g., Ryan & Dixon, 2008) to hundreds of km^2 (e.g., Benda et al., 2003). Rarely are studies conducted in large rivers with greater than 1,000 km^2 drainage areas; for example, two studies after the Las Conchas fire in New Mexico, USA looked at changes in water quality (Reale et al., 2015) and fish assemblages (Reale et al., 2021) between lower-order streams near the fire and the mainstem Rio Grande (~30,000 - 40,000 km^2 drainage areas). This thesis is unique in that it is concerned with post-fire impacts on a fourth through sixth order river with drainage areas between 450 and 3,970 km^2.

Benda et al. (2003) studied enlarged alluvial fans at tributary junctions in 3rd through 6th order streams due to post-fire sedimentation in Idaho, USA and observed a complex response of fan deposition that included knickpoint creation at the toe of the fan, increased gradient downstream, decreased gradient upstream, and changes in the spatial distribution of channel substrates. In a study of one headwater and one higher order basin (4 and 25 km^2 drainage areas, respectively) that burned in the same fire, Ortega-Becerril et al. (2024) found the lower-order stream had a greater increase in transport capacity (measured by the ratio of post- to pre-fire shear stress) than the higher-order stream. Initial hillslope erosion and debris flow activity were followed by deposition then erosion in higher-order stream segments. This mirrors the response to sediment release below a dam on the North Fork Poudre River, which occurred during a routine autumn drawdown. Widespread silt-to gravel-sized sediment deposition occurred in pools followed by erosion through the thalweg but not the marginal eddies (Wohl & Cenderelli, 2000). After a wildfire in a montane watershed in Wyoming, Ryan & Dixon (2008) observed an increase in suspended sediment in the first five years post-fire but did not observe an increase in bedload. In a study of several decades of streamflow, Loáiciga et al. (2001) found annual streamflow increases up to 20-30% during fire-impacted water years in a 272 km^2 watershed in the

Santa Monica Mountains of southern California, USA. On the contrary, Tomkins et al. (2008) found that wildfires had no detectable impact on surface runoff in large watersheds (>100 km^2) in Australia during the 3-year period post-fire. Additionally, Lane et al. (2006) measured discharge and suspended sediment in three watersheds in Australia after a severe fire in 2003 and found significant increases in annual flow for the smaller watersheds but not for the larger watershed (100 km^2), although it did not burn as intensely. It is clear that higher-order streams have a mixed response to wildfires due to the multiple variables in attenuating fluxes in lower-order streams.

Post-fire water quality fluxes also show spatial variation and have been studied at larger watershed scales. After a catastrophic wildfire in New Mexico, USA, turbidity increased in second-order streams but was minimal downstream in the mainstem Rio Grande (Reale et al., 2015). After severe wildfires in southern Alberta, Canada, Emelko et al. (2016) observed increased concentrations of phosphorus and noted that fine sediments from burned catchments containing high amounts of bioavailable particulate phosphorus persisted for 7 years post-fire in large, downstream rivers (550 and 800 km^2 drainage areas).

Post-fire alterations to riverine fluxes can lead to change in channel form downstream. In the 12 – 13 years after 1988 wildfires in Yellowstone National Park, USA, Legleiter et al. (2003) observed increased stream power leading to downcutting in higher-order streams, which they attributed to increased streamflow and decreased sediment supply. During the first five years following the 1988 Yellowstone fires, Minshall et al. (1997) found differences in responses between headwaters (first and second order) and intermediate (third and fourth order) streams; through embeddedness measurements, they suggested a pulse of fine sediments moved from burned watersheds into headwater streams and gradually into intermediate streams, and they observed a decrease in median substrate size in first- through third-order streams over the five-year study. They were surprised to find retention of fine-grained inorganic sediments (sand and silt) in headwaters and attributed it to continued input from burned hillslopes.

Lower-order headwater streams are typically erosional, transport reaches that effectively pass excess fluxes downstream to higher-order streams, which are more likely to be response or depositional reaches (Schumm, 1977). In other words, as the ratio of sediment supply to transport capacity increases downstream, rivers become transport limited, finer grained, and favor deposition (Montgomery & Buffington, 1997). Therefore, it is less likely to see post-fire sediment effects in higher-order streams because of attenuation and the reduction in relative size and importance of the burned area. At any point in the watershed, the degree of impact will reflect the balance between erosional force and increased sediment supply versus erosional resistance and accommodation space for water and sediment storage in higher-order river corridors. Wildfires disrupt this balance, and the watershed response will be reflected in the way fluxes are attenuated.

In montane watersheds, low gradient, wide, multithread reaches with well-connected floodplains disproportionately attenuate fluxes of flow, sediment, and nutrients by reducing longitudinal connectivity and increasing lateral and vertical connectivity (e.g., Wohl et al., 2022). These reaches, which are referred to as beads (as in beads on a string), typically have instream large wood, which increases transient storage of water, sediment, and particulate organic matter by obstructing flow and producing hydraulic resistance (Ader et al., 2021; Wohl & Scott, 2017), and/or past or present beaver activity. Logjams are also resilient to disturbances such as floods (Wohl & Scamardo, 2021). Like many watersheds in the US, loss of beaver (*Castor canadensis*) in the Poudre River watershed has greatly reduced the ability of beads to attenuate fluxes. In a study of three megafires in the northern Front Range (including the Cameron Peak wildfire), Fairfax et al. (2024) showed that riparian areas with beaver dams had significantly lower burn severity than areas without beaver ponds. Additionally, beaver ponds in burned areas are effective at storing post-fire sediments (Dunn, 2023). Active beaver complexes develop a feedback loop in which ponds inundate the valley bottom and raise the riparian groundwater table, which encourages more riparian vegetation, which the beavers use to build more dams on the

channel and floodplain, leading to a complex, hydraulically rough, multithread channel and pond complex that can extend the full width and length of the bead (Polvi & Wohl, 2012). Incision occurs when beavers are removed or a bead is channelized, which reduces floodplain connectivity, lowers the water table, and leads to loss of riparian vegetation (Wolf et al., 2007). This results in less attenuation of fluxes and lower resiliency overall.

1.2.2 Aquatic ecosystem response to wildfires

From loss of vegetation to effects on hydrology and water quality, wildfire effects can impact aquatic ecosystems, food webs, and ecosystem processes in a variety of ways and across a range of scales (Bixby et al., 2015). In a synthesis of wildfire-related literature, Gresswell (1999) suggests that stresses due to altered hydrology are probably the primary driver influencing persistence of fish, benthic macroinvertebrates, and diatoms in fluvial systems. At the base of the aquatic food web, fires indirectly affect benthic macroinvertebrates through increased streamflow and fine sediment (Minshall, 2003). For example, benthic macroinvertebrate composition, but not abundance, changed in the five years following the 1988 wildfires in Yellowstone National Park (Minshall et al., 1997). Other ecosystem responses to the Yellowstone fires included increased water temperatures and nitrogen levels, an increase in wood recruitment in lower-order streams, and increases in several types of organic matter (Minshall et al., 1997). Aquatic fauna are affected by a range of post-fire conditions such as increased light and water temperature, ash toxicity, increased turbidity, changes to nutrients, and natural and human-made chemicals (Gomez Isaza et al., 2022). After the 2011 Las Conchas wildfire in New Mexico, USA, a study at two sites on the mainstem Rio Grande (29,000 and 36,000 km^2 drainage areas, respectively) showed that in lower-order streams, fish assemblage was suppressed following a major flood event two years post-fire, but overall, fish species richness and evenness were not strongly affected by the wildfire (Reale et al., 2021). Figure 1 shows projected stream ecosystem response of several ecological indicators following a wildfire (from Minshall et al., 1989; Figure 2).

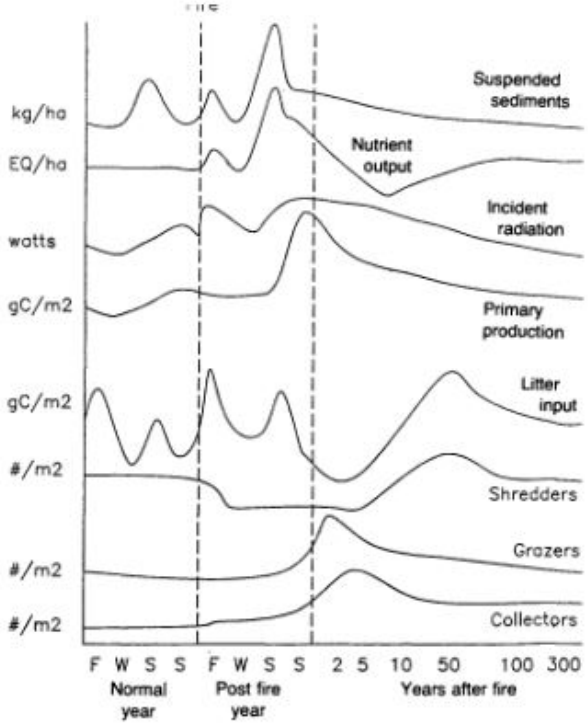

Figure 1. Projected stream ecosystem response to a wildfire. From Minshall 1989, Figure 2.

Regardless of the source, elevated fine sediment is a major cause of habitat loss and ecosystem destruction, especially for salmonids. Increased sediment yield has been shown to fill pools in gravel/cobble bed pool-riffle channels, which decreases the volume of the pools at low flows and reduces habitat (Lisle & Hilton, 1992). Excess fine sediment can also increase riffle surface fine sediment and decrease spawning gravel permeability, reducing the abundance of benthic macroinvertebrates upon which salmonids prey (Cover et al., 2008). Kemp et al. (2011) summarizes the impacts of excess fine sediment to riverine fish in three major ways: 1) fine sediment can impact fish physiology and performance by directly damaging organs or indirectly influencing water quality; 2) increased fine sediment concentrations and turbidity impacts fish behavior by reducing visibility for visual foragers, impairing visual communication for courtship, communicating with young, or hinderance of fish migration; and 3) deposition of fine sediment impacts fish habitat by filling in or covering up spawning gravels, thus reducing potential for survival of eggs, which have specific hydraulic and substrate

conditions necessary for survival (primarily for salmonids), and infilling of interstitial space and vegetation loss can lead to reduction of cover for juvenile salmonids to avoid predation.

1.2.3 Flushing flows

River ecosystems are inextricably linked to the natural flow regime, which is the unique pattern of variation and timing of flow throughout a year (Poff et al., 1997). Several human alterations directly or indirectly modify the flow regime, subsequently impacting geomorphic processes and aquatic ecosystems. For example, Graf (2006) found that on large American rivers, areas downstream of dams have reduced peak flows, flow variability, floodplain area, and geomorphic complexity. Functional flows are flows that serve ecological purposes (Escobar-Arias & Pasternack, 2010) and can be initiated in regulated rivers to mimic elements of the natural flow regime (Yarnell et al., 2015). Common functional flows include peak magnitude flows and dry-season base flows. Implementation of functional flows in regulated rivers has been shown to benefit native fish populations (e.g., Marchetti & Moyle, 2001; Propst & Gido, 2004).

Another impact of flow regulation is the alteration of the natural sediment regime (Wohl et al., 2015). Dams and diversion structures block the longitudinal mobility of sediments and reduce the sediment supply downstream, which can cause incision downstream and impact lotic ecosystems.

Flushing flows are specific instream flows that perform a particular ecological or management objective by mobilizing or removing sediment from a given river (Kondolf & Wilcock, 1996). Common objectives include restoring and enhancing riffle or pool habitat, maintaining active channel width and topography, creating or building floodplain habitats, and creating diverse multiage riparian habitats. Each objective has a particular flow requirement for mobilizing a portion of the substrate, transporting material out of a given reach, depositing fine sediment, or eroding banks. Specific sediment mobilization

objectives commonly have a particular species or habitat in mind, such as cleaning spawning gravel for salmonids or removal of interstitial fine sediment for benthic macroinvertebrates.

Flushing flows can be calculated using hydrological methods, effective discharge, and empirical flushing flow functions developed for different sediment flushing scenarios (e.g., Milhous, 2019). In streams impacted by excess fine sediment, the flushing flow objective may be to mobilize the coarse bed material, which should also flush the fines from the substrate. This entrainment threshold is usually defined by a critical shear stress or velocity that mobilizes some or part of the bed material (Dey & Ali, 2019). Shields (1936) developed a commonly used formula for critical shear stress required to initiate mobilization of uniform sediments, but substrate in rivers usually has mixed grain sizes. Empirical formulae have been developed to determine entrainment thresholds of a desired portion of the substrate (D_i) relative to median grain size (D_i/D_{50}) (e.g., Andrews, 1984; Komar, 1987). Additionally, in unimodal sediment mixtures, critical shear stress for any fraction of the mixture depends on the mean grain size (Wilcock, 1993), so in many cases it is practical to use the critical shear stress of the median grain size (D_{50}) of the substrate to estimate entrainment thresholds of a gravel bed river (Wilcock et al., 2009). In bimodally distributed sediment mixtures, which may have a primary mode in the gravels and secondary mode in the sand sizes, hiding functions reduce the mobility of the smaller grains, so critical shear stress can be estimated using relative grain-size functions (e.g., Wilcock & Crowe, 2003).

2.1.1 Poudre River watershed

The Poudre River watershed (Figure 2) encompasses 4,895 km^2 in the northern Front Range of northern Colorado and southern Wyoming. The Poudre River begins at the continental divide in western Larimer County at 4,145 m elevation and joins the South Platte River near Greeley, CO at 1,399 m elevation. The Poudre River watershed is underlain by Precambrian metasedimentary and metaigneous rocks of the northern Front Range and by Pleistocene alluvium in the plains. Tilted Pennsylvanian through Cretaceous sedimentary beds form the piedmont between the mountains and the plains (Workman et al., 2018).

In the study area, the Poudre River has two distinct fluvial regions and flow regimes – upstream canyon reaches are laterally confined alluvial and bedrock channels with moderate to high gradient and a cobble and gravel substrate, while the downstream transition zone is characterized by lower gradients and gravel substrate and is where the river transitions to a typical fine-grained substrate Great Plains-type river. In this study, the transition zone is defined as the area between the canyon mouth at Bellvue, CO (Canyon Mouth gauge labeled "CN" in Figure 2), to where the Poudre River crosses Interstate 25 downstream of Fort Collins, CO. The interstate does not mark a distinct fluvial boundary, but it is commonly used to classify this reach. The transition zone river reach historically had multi-thread, sinuous channels with broad floodplains but has been confined to a rigid, single-thread system due to urbanization and development in the 20th century (Figure 3, Bestgen et al., 2020; Shanahan et al., 2014). Since the 1930's, sinuosity has decreased while wavelength has increased due to channelization (Sexton, 1998). In this study, the drainage area ranges from 450 km^2 for the upstream sites to 3,970 km^2 at the downstream sites and the Poudre River is a fourth- through sixth-order river.

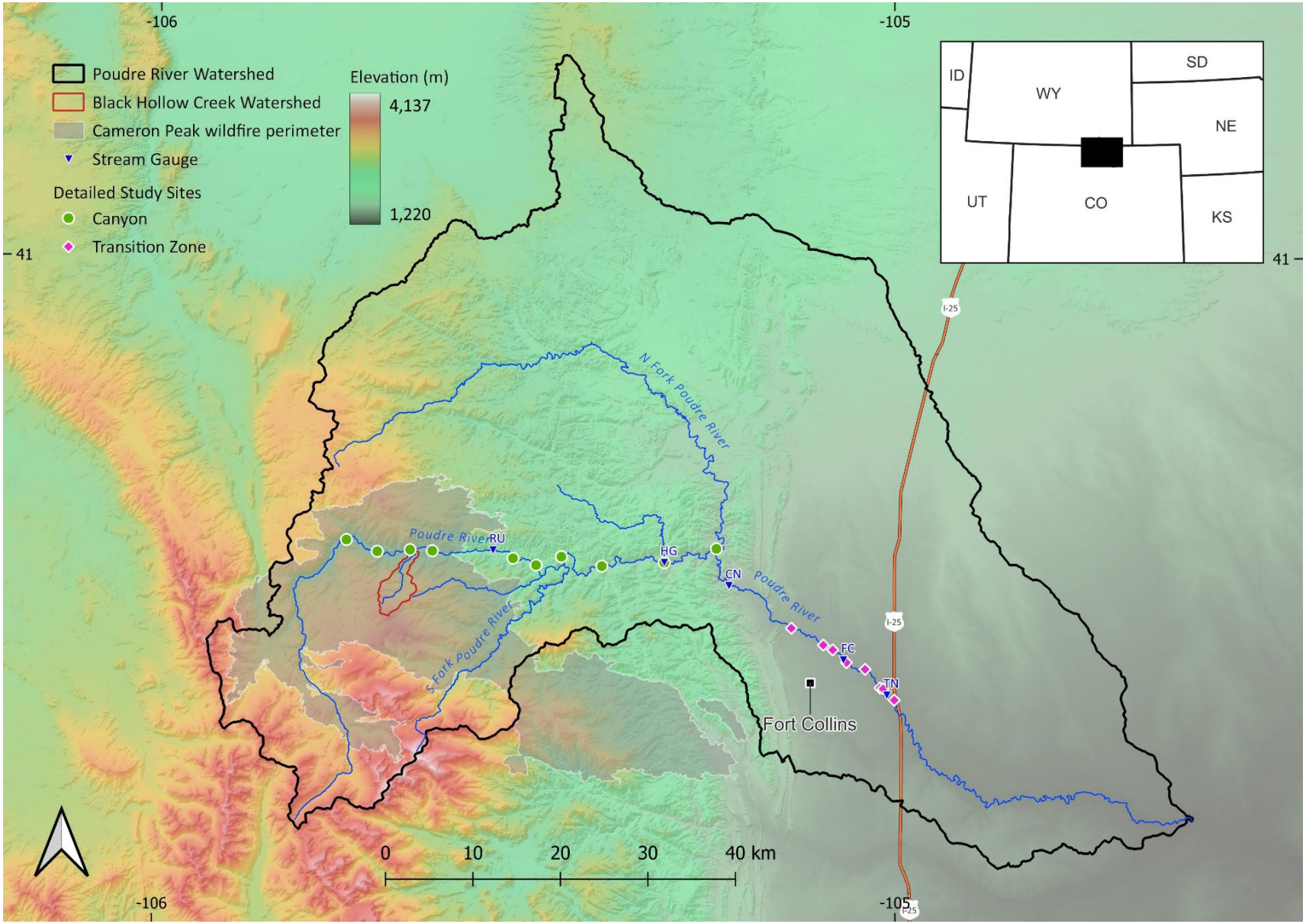

Figure 2. Poudre River watershed and detailed study sites. Stream gauges: RU: Rustic; HG: Hewlett Gulch; CN: Canyon Mouth; FC: Fort Collins; TN: Timnath.

a) 1937

b) Recent, circa 2005

Figure 3. A 2.5 km long reach of the Poudre River in Fort Collins, CO, downstream of Lions Park (a) in 1937 and (b) 2005. (a) shows a multithread, laterally unconfined channel with an active and accessible floodplain, while (b) shows a confined, leveed, single thread channel with little lateral mobility, floodplain, or riparian forest. Flow is left to right in each image. From Bestgen et al. (2020) Figure 2

Precipitation primarily falls as winter snow and summer rain during convective storms. The City of Fort Collins receives on average 383 mm of precipitation per year (National Oceanic and Atmospheric Administration, 2024). The flow regime of the Poudre River consists of a snowmelt-dominated spring peak, summer convective storms capable of producing large floods at lower elevations (below 2300 m; Jarrett, 1990), and winter base flow. Although no major dam exists on the mainstem Poudre, numerous diversions for agricultural and municipal use reduce peak and base flows from pre-development levels by 59% and 57%, respectively (Shanahan et al., 2014). Reduction in high flows that mobilize cobbles and gravels has led to armoring, or the coarsening of the substrate, and to the filling of interstitial space with

fines (Shanahan et al., 2014). The canyon zone maintains a somewhat more natural flow regime because most diversion structures occur in the transition zone. Figure 4 shows differences in discharge throughout a typical year (2021) between two canyon gauges, Hewlett Gulch and Canyon Mouth, and the Timnath Gauge, downstream of Fort Collins.

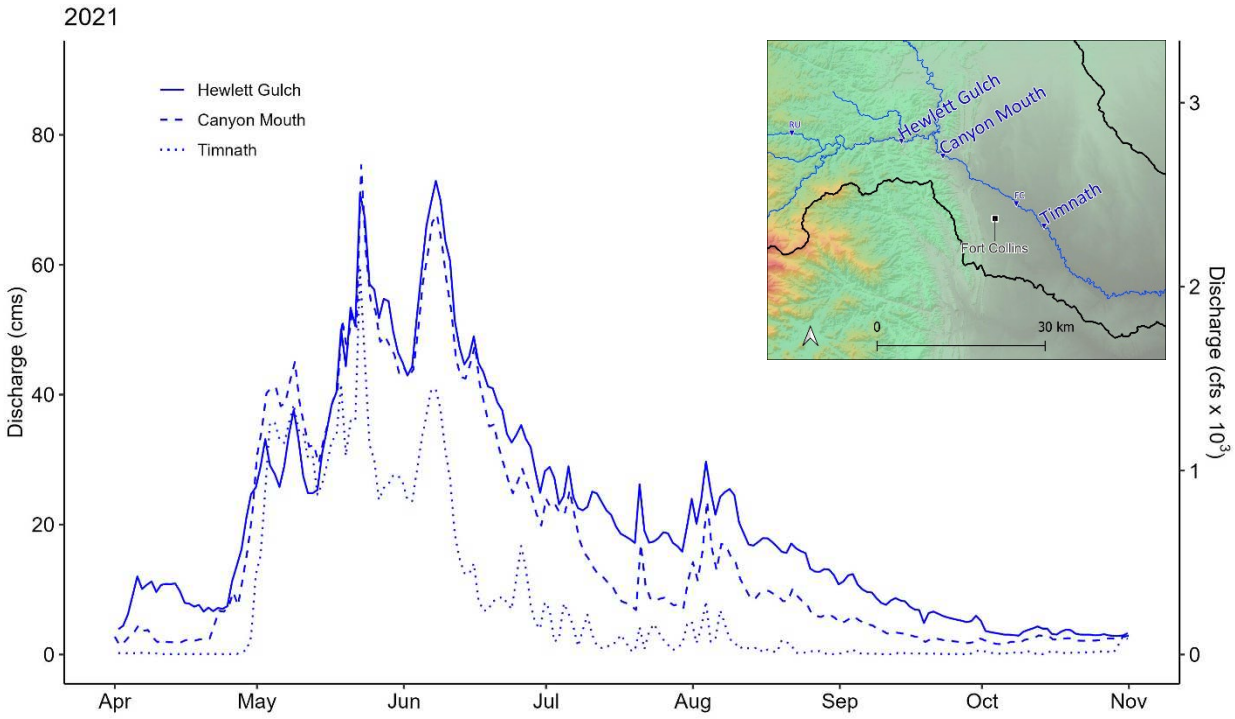

Figure 4. Hydrographs at three Poudre River stream gauges. Data from USGS, CO DWR, and Larimer County.

The City of Fort Collins' "State of the Poudre River", a cumulative assessment of Poudre River health in the transition zone, gave the river an overall grade of C, indicating that the river supports "basic elements of a functioning river ecosystem," despite alterations and degradations by local and system-wide stresses (City of Fort Collins, 2017). The report notes that channelization, bank armoring, gravel mining, and other infrastructure restricts floodplain access in the upstream portion of the transition zone, while some accessible floodplain exists downstream in conserved open lands. The transition zone has both points of water extraction at diversion structures and inflows used to convey water downstream, which lead to unpredictable flows that can be harmful to aquatic ecosystems.

The transition zone is the western-most extent of many Great Plains fishes (Fausch & Bestgen, 1997), and since the 1990s native fish species diversity, distribution, and abundance have declined, partially due to water diversions and increased presence of non-native brown trout (*Salmo trutta*) (Haworth & Bestgen, 2024). The transition zone spans the gradient between cold, trout-dominated waters to a mixed temperature regime with warmwater plains fishes downstream.

2.1.2 Cameron Peak wildfire and the Black Hollow debris flow

The Cameron Peak wildfire of 2020 burned over 84,000 hectares (840 km^2) in Colorado's northern Front Range and is, to this day, the largest wildfire in State history. In the Poudre River watershed, the fire burned 558 km^2. The fire burned high elevation forests that do not commonly experience fire. High mortality of trees due to bark beetles combined with high temperatures, low humidity, and gusting winds led to rapid spreading and extreme fire behavior. Post-fire soil burn severity mapping indicates 20% of the burn was very low/unburned, 44% burned at low severity, 30% burned at moderate severity, and 6% was burned at high severity (BAER, 2020). Most of the fire burned in the headwater tributaries, the South Fork, and along the mainstem of the Poudre River. Approximately 266 km of perennial streams experienced fire nearby (Fairchild, 2021).

Due to the burn severity and steep slopes of the burned area, many burned watersheds had a high probability of experiencing a debris flow (Kostelnik et al., 2021). Within the Cameron Peak wildfire perimeter, 88% of the burned area was given an erosion hazard rating of moderate or severe. Ninety percent of the Black Hollow watershed burned during the Cameron Peak wildfire (Fairchild, 2021), and several of its sub-basins were assessed to have greater than a 40% chance of debris flow activity (Kostelnik et al., 2021).

Recent studies of the Cameron Peak wildfire and its effects indicate alterations to several watershed processes that could have downstream effects. McGrath et al. (2023) observed reduced snow water

equivalent and elevated snowmelt rates in high burn severity forests within the burned area. Miller (2022) found that high elevation sites within the Cameron Peak Fire were more responsive to rainfall in producing a streamflow response compared to other elevations. Miller also noted that in both persistent (deep snow persists throughout the winter) and intermittent (continual snow cover occurs periodically throughout the winter) snow zones, unburned sites produced less streamflow response to summer rainfall events. Wohl et al. (2024) found that a wildfire-related debris flow and flood caused significant changes to logjam distribution in a tributary to the South Fork Poudre River burned in the Cameron Peak wildfire. In a study of high elevation stream-riparian food webs following three large wildfires in the northern Front Range (including the Cameron Peak wildfire), Preston et al. (2023) showed reduced benthic macroinvertebrate density and flux of emerging aquatic insects in burned streams compared to unburned streams as well as some evidence for reduced trout abundance in burned streams. They observed larger fish and an absence of young fish at burned sites, potentially indicating that large fish are more resistant to fire-associated disturbance or that large fish re-colonize burned areas after a population decrease. Watershed-scale water quality impacts associated with increased erosion were seen in the Poudre River, including elevated background levels of turbidity, total dissolved solids, nutrients, and total nitrogen (Heath & Thorp, 2023). Water quality impacts still occur during the summer monsoon season in severely burned areas, such as the North Fork Big Thompson River (Loveland Power and Water, 2023).

On 20 July 2021, a convective storm over the burn scar triggered a massive debris flow in Black Hollow canyon that resulted in four fatalities and deposited significant amounts of sediment, ash, and large wood along the mainstem Poudre River. A mix of sediment sizes from fines to boulders were deposited at the mouth of Black Hollow, and the debris fan formed a large pool upstream (Figure 5). Toxic levels of sediment and ash in the river reduced oxygen levels, leading to a massive fish kill (Figure 5C, 5D, and 5E). Sampling in 2021 after the debris flow by Colorado Parks and Wildlife (CPW) indicated a

complete loss of the fishery between Black Hollow and Stove Prairie (32 km downstream), with fish populations returning to normal levels at Lions Park (65 km downstream). In total, impacts to the fishery occurred over 95 km downstream from Black Hollow (Battige, 2022). The surge of debris and sediment required the City of Fort Collins to shut down water intakes on the Poudre River, and elevated turbidity continued to pose threats to water treatment for several weeks (Heath & Thorp, 2023).

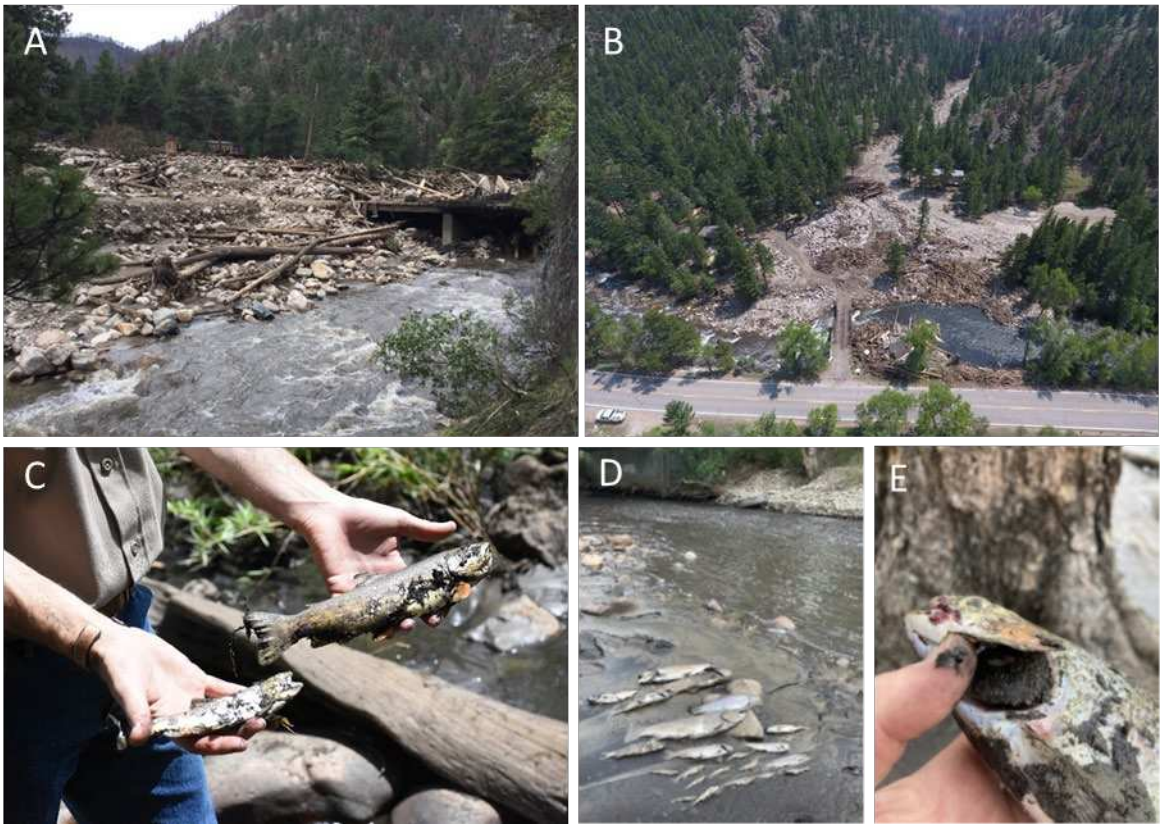

Figure 5. (A) & (B) Debris fan at junction of Black Hollow and Poudre River. Photos courtesy of Ayres Associates. (C), (D) & (E) Fish kill from toxic levels of sediment and ash after the Black Hollow debris flow. Photos courtesy of CPW.

The flood pulse from the Black Hollow debris flow can be seen in Figure 6, which plots the 2021 hydrographs from five stream gauges on the mainstem Poudre River. At the Rustic gauge, 12 km downstream of Black Hollow, the flood pulse peaks around 60 m^3/s and is considerably higher than the peak snowmelt runoff. At Hewlett Gulch, 42 km downstream, it registers as a significant peak at 40 m^3/s, but less than the peak snowmelt runoff. At the canyon mouth, Fort Collins, and Timnath gauges, the flood pulse decreases in magnitude and registers similarly to other late summer and fall peaks.

Although the flood was attenuated by the time it reached the transition zone, the sediment pulse was easily transported downstream. Immediately after the Black Hollow debris flow, significant fine sediment deposition occurred throughout the transition zone, primarily in backwaters and upstream of diversion dams but also in the active channel and lateral margins (M. Haworth, personal communication, April 2024). For example, Figure 7 shows the filling of an approximately 50 m long backwater with sand after the Black Hollow debris flow at site T06 in Fort Collins. After spring runoff in 2022, most of the very fine material was remobilized from the active channel areas, but sand was retained. Depositional areas, such as backwaters and areas upstream of diversion dams, continued to accumulate fines even as high flows receded. Depositional areas continue to retain fines at the time of this writing.

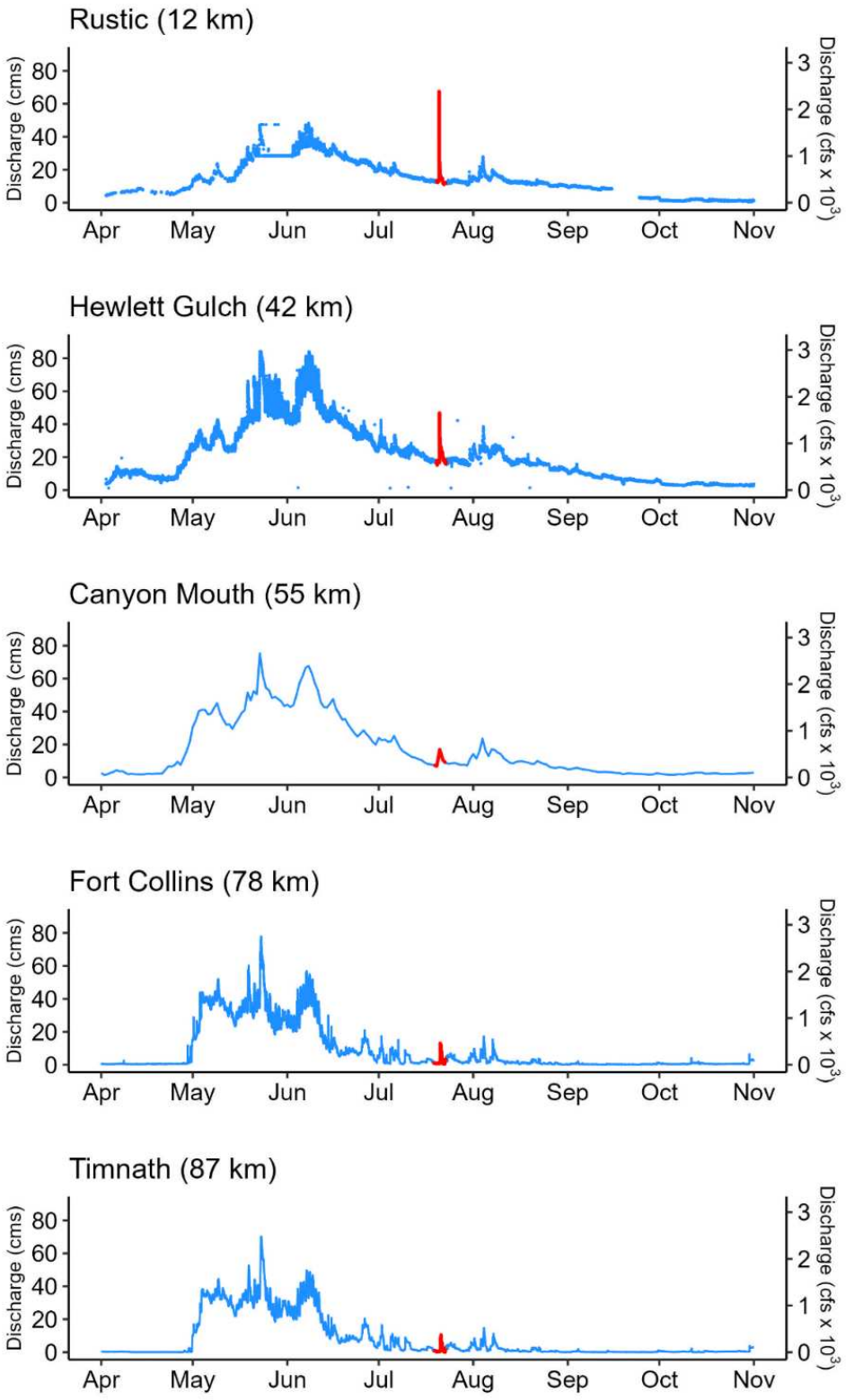

Figure 6. 2021 Hydrographs at five Poudre River stream gauges and distance downstream from Black Hollow confluence. Flood pulse caused by the Black Hollow debris flow shown in red. Gauge locations shown in Figure 2.

Figure 7. Fine sediment deposition in backwater and margins at site T06 in Fort Collins. Arrow indicates flow direction.

3. METHODS

3.1 Site Selection

Eighteen detailed study sites were chosen to overlap with existing fish population monitoring sites operated by Colorado Parks & Wildlife (CPW) and Colorado State University (CSU) (Figure 8, Appendix). CPW monitors 12 sites spanning from Kinikinik to Fort Collins and CSU monitors 13 sites in the transition zone. Fish monitoring sites are usually no more than 300 m long. For this study, study sites are all approximately 300 m long and span several habitat units (riffle, run, pool, etc.). Sites beginning with "T" are CSU fish monitoring sites.

Originally, a total of 16 sites were chosen, including 8 sites in the canyon (3 of which are upstream of Black Hollow) and 8 sites in the transition zone. Because the canyon section encompasses more river length, I added two sites (Dutch George and Hewlett Gulch) in areas of the canyon that had less coverage for a total of 18 sites.

Four sites were selected for hydraulic modelling of bed mobilization that represent different geomorphic settings throughout the study area. The four sites included one upstream of Black Hollow (Pasquinels Cabin), one downstream of Black Hollow in the canyon (Indian Meadows), and two in the transition zone: Shields Street (T03) and the Archery Range (T12). Shields Street is a channelized, bank stabilized, and relatively high gradient (for the transition zone) reach with low fine sediment volume but high embeddedness. The Archery Range is the farthest downstream reach with a low gradient, high fine sediment volumes, and high embeddedness. At this site, many of the backwaters, side channels, and marginal eddies are infilled with large sand deposits. Comparing thresholds of bed mobilization between the four sites may help explain sediment retention trends throughout the study area.

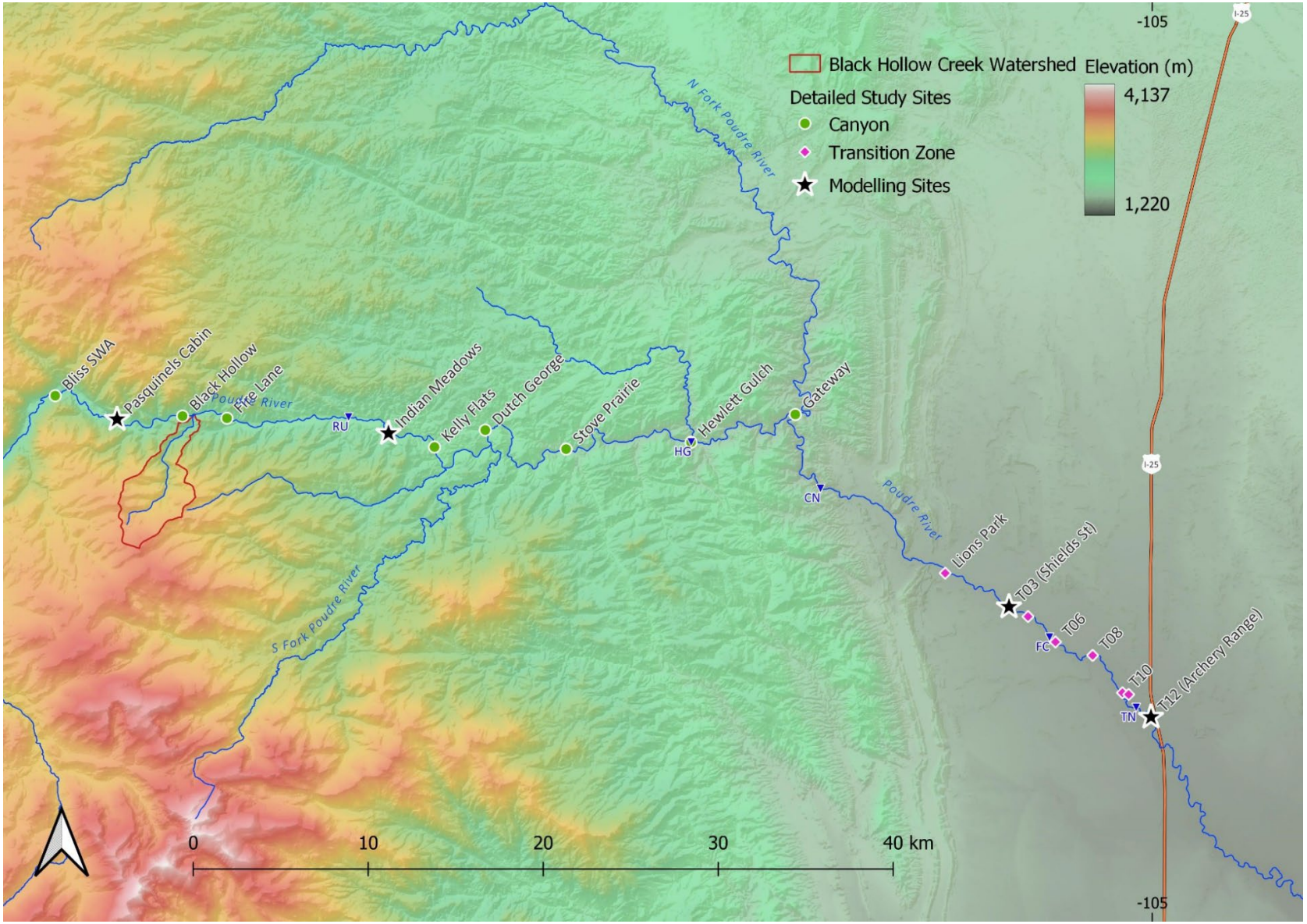

Figure 8. Detailed study sites. Stream gauges: RU: Rustic (City of Fort Collins); HG: Hewlett Gulch; CN: Canyon Mouth (CO Division of Water Resources); FC: Cache La Poudre at Fort Collins (USGS); TN: Cache La Poudre above Boxelder Creek (USGS).

3.2 Volumetric Surveys

The first sediment retention metric is the volume of fine sediment deposits normalized to the bankfull volume of each reach (fine sediment volume (m^3)/bankfull volume (m^3)). Only deposits below the bankfull line were measured, and I attempted to differentiate recent deposition due to the Cameron Peak wildfire and Black Hollow debris flow from other fine-grained areas based on amount of vegetation and presence of ash and charcoal.

I chose to measure deposits longer than 5 m to capture deposits that may remain in place in the near future. To calculate volume, I measured the length of the long axis, which usually was parallel to the river, and width at roughly 10 evenly spaced perpendicular transects. At each transect, I took three depth measurements at 25%, 50%, and 75% of the width with a metal rod until hitting refusal from coarse-grained material or a pre-existing layer. I calculated the volume of each deposit by multiplying the trapezoidal cross-sectional area by the planimetric area of each transect and summing them.

3.3 Transect Surveys

Transect surveys were conducted to characterize channels at a smaller scale. Surveys were based on physical habitat surveys that CSU conducts during their fish sampling, with some additional metrics. Transects spanned the bankfull channel width and were spaced one tenth of the reach length, or every 30 m. Each transect was categorized into a bedform of either riffle, run, pool, side channel, or backwater. Side channels are channels that are separated from the active channel by an area above bankfull (island) that is inundated some part of the year. Backwaters are off-channel areas that are usually inundated at low flows and are connected to the active channel. They are distinguished from side channels by being inundated via backfilling from the main channel, whereas side channels have a surface connection from upstream. This allows analyses of fine sediment retention by channel unit.

3.3.1 Embeddedness

The degree of embeddedness was visually estimated at 5 evenly spaced points along each transect. A modified approach based on the US EPA's Environmental Monitoring and Assessment Protocol was used (Peck et al., 2001). Embeddedness was quantified into quartile percentages (0%, 25%, 50%, 75%, and 100%) based on visual estimation and inspection of individual large grains at each point along the transect. For example, 25% embeddedness means that 25% of an individual coarse grain is surrounded by fine sediment, and 100% means that the coarse grains are completely covered. Averages were calculated for each transect and each site.

Limitations arise from this method because it is relatively subjective. Measures were taken to reduce the number of people making measurements to decrease person-to-person variability. If repeat surveys are conducted, it is important to follow the same protocol.

3.3.2 Sediment size

Sediment size was visually estimated at the same 5 evenly spaced points. Continuing with the CSU habitat survey method, sediment size was grouped into classes and listed in order of decreasing abundance. Sediment classes included fines (<0.06 mm), sand (0.06 – 2 mm), gravel (2 – 64 mm), small cobble (65 – 128 mm), large cobble (129 – 256 mm), and boulders (>256 mm). Values at each point included up to three sediment classes, listed by primary, secondary, and tertiary abundance (e.g., cobble, gravel, sand). Each survey point, which consisted of one to three sediment size classes, was averaged using the central value of each class to yield 55 values, and the median grain size (D_{50}) was determined from those values.

3.3.3 Cross-sectional geometry

Cross-sectional geometry was measured in two ways: using an auto-level and stadia rod or using an RTK GPS. The RTK was not functional in some canyon reaches due to lack of satellite availability. Both methods were surveys of the bankfull channel topography and bathymetry at each transect.

A set of Emlid Reach RS2 RTK GPS receivers were used at some of the sites. One unit was the local base station, and the other was the rover to collect points. The survey data were post-processed using NOAA Continuously Operating Reference Stations (CORS) correction and Emlid Flow software. Geographic coordinates (northings and eastings) were converted into distance along the transect (station) using the Pythagorean theorem to plot cross sections and match them with the auto-level/stadia rod surveys, which were in station-elevation format.

I entered the survey data into Cross Section Viewer (Shelley & Bailey, 2018), a software that calculates cross-sectional geometries such as bankfull width, bed length (bankfull wetted perimeter), cross-sectional area, average channel elevation, max depth, and others. With these data, I calculated hydraulic radius (cross-sectional area/bed length) and width-to-depth ratio (bankfull width/average depth) for each transect and averaged them for each site.

3.4 Geospatial Analysis

3.4.1 Basin-wide analyses

I conducted desktop spatial analyses in QGIS (version 3.26.3). To calculate distances along the Poudre River, I used the QChainage tool in QGIS to create points along the river centerline 100 m and 1 km apart and labeled them appropriately. I chose the confluence with Black Hollow as 0 km, so the three sites upstream have negative distance values.

To create a longitudinal profile of the Poudre River, I used the Profile Tool in QGIS that plots a profile of a selected line vector and the corresponding heights of an elevation raster, which was a USGS 10-m digital elevation model (DEM).

3.4.2 Reach scale analyses

Gradient: I calculated the channel gradient using the bed elevations from the RTK or auto-level surveys and thalweg length from QGIS.

Bankfull Area (planimetric): I delineated the bankfull boundary using LiDAR DEMs and aerial imagery in QGIS. I created a bankfull area polygon using the polygonize tool, subtracted any islands above bankfull with the Difference tool, and calculated the remaining area with the Field Calculator in QGIS.

Bankfull Width: I first calculated bankfull width by dividing the planimetric bankfull area by the centerline distance. I also averaged the measured bankfull widths from the transect surveys, which yielded similar results.

Bank Length Ratio: Bank length ratio is the ratio of the total bank length to the centerline length in a given reach (Polvi et al., 2014). A perfectly straight channel with straight banks will have a value of 2 and banks with irregularities will have higher values. Besides the outer banks, bank lengths of islands are included in the numerator. I delineated bankfull lines in QGIS to calculate the total bank length at each site and divided it by the centerline length.

3.4.3 DEM creation for hydraulic modelling (canyon sites)

At the two canyon sites selected for hydraulic modelling (Pasquinel's Cabin and Indian Meadows), I combined bathymetric RTK surveys with 1 m resolution LiDAR into a single DEM to use for hydraulic modelling. Airborne LiDAR lasers emit a near-infrared wavelength of 1064 nm for terrestrial purposes but are unable to scan beneath water surfaces. Typically, DEMs created from LiDAR are "hydro-

flattened" – meaning the elevations of a water body are the water surface, which is not feasible for hydraulic modelling. Bed elevations of submerged areas can be obtained with instruments such as bathymetric LiDAR (532 nm wavelength), sonar, or acoustic Doppler current profiles for finer spatial resolution, or manually with GPS devices, such as an RTK.

I obtained both raw LiDAR point cloud files and DEMs for each site from the USGS 3DEP website. Using a combination of hillshade, profile tool, and slope raster of the DEM, I created a polygon of the flattened water surface on the DEM in QGIS. In CloudCompare (version 2.11) software, I cut this area from the ground points of the LiDAR point cloud using the Segment tool. I created a mesh of the bathymetric points with the Rasterize tool and cut that to the water surface polygon. Finally, the two point clouds were combined into a single point cloud using the Merge tool and rasterized into a 1 m resolution DEM using the Rasterize tool. Note that the bathymetric portion of the resulting DEM does not have the resolution of the terrestrial portion of the DEM because it was interpolated between cross sections.

3.4.4 Drone surveys (transition zone sites)

The low cost and easy access to recreational grade uncrewed aerial vehicles (UAVs or drones) coupled with user friendly SfM software has allowed researchers and professionals of many fields to produce high-resolution datasets for a variety of applications (Westoby et al., 2012). Drone-produced SfM products such as DEMs and orthomosaic images have several applications in fluvial and aquatic studies (Carrivick & Smith, 2019). Commonly used products include topographic and bathymetric surveys, geomorphological mapping and change detection, grain-size mapping, vegetation mapping, restoration monitoring, habitat classification, and sediment transport path delineation.

Drone surveys were conducted at site T03 (Shields Street) and T12 (Archery Range) to create DEMs for hydraulic modeling. The available LiDAR DEMs of the area from 2013 are outdated because the channel has shifted significantly in the past decade.

I rented a Parrot ANAFI Ai drone from the CSU Drone Center for the surveys and flew Shields Street and the Archery Range on 5 and 6 December 2023, respectively. I placed nine ground control points evenly spaced throughout each survey area (GCP) and surveyed them with an RTK. The flights were conducted near solar noon for optimal lighting conditions. The drone was flown 60 m above ground level (AGL) from the take-off location. Equipped with a 48-megapixel camera, the drone uses Free Flight 7 software to plan an automatic flight path; for 3D reconstruction like SfM, it flies a cross-hatched flight pattern with a camera angle of 70 degrees from horizontal. Due to the rectangular survey areas, the flight paths were perpendicular crosshatches, and the camera took one picture every 5 seconds on the short axis, and one picture every three seconds for the long axis to achieve 70% side and 80% front overlap between pictures.

I also surveyed bathymetry with the RTK to test the reconstruction of the underwater areas. Because light refracts through the water column, I expect that SFM models of submerged areas will be inaccurate, with water depths appearing shallower than they are. For example, Dietrich (2017) calculated a series of refraction correction equations for each point/camera combination in a SfM point cloud. In shallow water reef environments (less than 1 m deep), David et al. (2021) found that they could accurately reconstruct the bathymetry with a combination of subaerial and submerged GCPs, and that errors in the DEM increase with increasing water depth. In another case, Woodget et al. (2017) measured the errors from drone-based SfM elevation models in exposed and submerged areas along the River Teme, UK, and found mean elevation error of 0.052 m for exposed areas, and 0.101 m for submerged.

Aerial images from the flights were processed in Agisoft Metashape (version 1.5.2). Metashape creates tie points by finding the same point on two or more images, and then aligns the cameras based on the points. It first creates a sparse point cloud, which is then used to create a dense point cloud. The dense point cloud is then classified into ground points using the Classify Ground Points tool. Metashape can then create a DEM of the ground points, but it did not "see" beneath some trees on the bank, and I needed to remove a bridge at the Archery Range site. I made fine-scale adjustments to the point cloud in Cloud Compare. To clean up areas with trees overhanging the water surface, I first cut out the channel bottom from the point cloud, including the problem area. Then, I cut out the problem area from the first cutout and interpolated the area using the rasterize function, before combining the initial cutout back into the original point cloud. I followed a similar procedure for removing the bridge at the Archery Range site.

In Metashape, dense point clouds were created with six of the nine GCPs in the model creation, along with several bathymetric RTK points acting as GCPs. Although these points were not true GCPs with targets to match between photos (as in David et al., 2021), their inclusion in the dense point cloud creation yielded more accurate results. The final DEMs and orthophotos had spatial resolutions of 0.03 and 0.01 m, respectively.

At the Archery Range, the median difference between surveyed RTK points of the submerged area and the resultant DEM was very low (median = 0.010 m, mean = 0.032 m, n = 111; see Appendix), but the near-zero differences can be misleading. When plotted against each other, the best fit line had a slope of 0.76 and R^2 of 0.88. The plot shows overestimations of bed elevations at lower elevations and underestimations at higher elevations. At Shields Street, the overall differences were higher (median = -0.058 m, mean = -0.068 m, n = 111; see Appendix), but the expected versus modelled elevations were more accurate (slope = 0.85, R^2 = 0.94). Without using a refraction correction, the bed elevations were

accurate enough to run hydraulic models without issue once calibrated. See Appendix for accuracy metrics.

3.5 Statistical Analyses

Statistical analyses were performed in R Statistical Software (version 4.2.2, R Core Team, 2021). To determine drivers of fine sediment volume and embeddedness, I used linear regression techniques on the predictor variables. I performed a base-10 logarithmic transformation on the volume and embeddedness to achieve normal distributions. The reach location variable is a categorical indicator which categorizes sites as control (upstream of Black Hollow; n = 3), canyon (downstream of Black Hollow within the canyon zone; n = 7), or transition zone (n = 8). Splitting the canyon sites upstream and downstream of Black Hollow can reveal whether the debris flow had noticeable effects on fine sediment retention. Reach scale predictor variables to test include bed gradient, average width-to-depth ratio, average cross-sectional area, and bank length ratio.

The volume metric was averaged over each site, while embeddedness was averaged over both the site and by transect. This allows a test of embeddedness as a function of transect-level variables. These include bedform (habitat unit), cross-sectional area, and width-to-depth ratio. The transect-level data included a full dataset (n = 213) and dataset of only main channel bedforms (n = 185), excluding side channels and backwaters. In both datasets, embeddedness distribution appears normal based on visual observation of histograms and quantile-quantile plots.

Tables 1 & 2 explain the variables used in statistical tests and list the objectives and statistical tests used in the multiple linear regression, respectively.

Table 1. Explanation of response and predictor variables used in multiple linear regression.

Variable	Abbreviation	Units	Notes
Response			
Volume of fines per bankful volume	Volume	m^3/m^3	total site volume divided by site bankfull volume (average XSA x reach length)
Embeddedness	Emb	%	averaged from approx. 55 samples per site
Predictor - distance downstream			
Distance downstream of Black Hollow	Dist_BH	km	site upstream of BH are negative values
Reach location	location	NA	categorical - groups based on geomorphic setting: upstream of BH, downstream of BH in canyon, transition zone
Predictor - site-specific			
Channel gradient	grad_bed	m/m	gradient of channel bed
Width-to-depth ratio	WDR	m/m	bankfull width divided by average depth at each transect, averaged by site
Cross-sectional area	XSA	m^2	calculated for each transect, averaged by site
Bank length ratio	BLR	m/m	total length of banks divided by centerline distance
Predictor - transect			
Bedform	Bedform	NA	categorical

3.5.1 Regression of fine sediment volume by site

To determine the relationships between volume and predictor variables, while specifically comparing between distance downstream and reach scale variables, I compared linear regression models with different predictor variables. To directly test the relationship effect of distance downstream, I conducted an Anova test of $\log_{10}$(volume) against reach location, which is a categorical indicator of distance downstream. Sites were categorized as control (upstream of Black Hollow; *n* = 3), canyon (downstream of Black Hollow within the canyon zone; *n* = 7), or transition zone (*n* = 8). Then, to compare all possible combinations of predictors, I used the *dredge* function from the MuMIn package (version 1.47.5, Barton, 2023) that ranks every possible model based on corrected Akaike's Information Criterion (AIC_c; corrected for smaller sample size), which ranks all possible models for a dataset. I input a full model into the *dredge* function containing all predictor variables: reach location (location), gradient (grad_bed), cross-sectional area (XSA_ave), width to depth ratio (WDR_ave), and bank length ratio (BLR). The output lists all possible models from most supported (lowest AIC_c) to least. Models with less than or equal to two AIC_c units (Delta AIC_c) from the top model were interpreted to have substantial

support (Burnham & Anderson, 2002). This model selection technique was run with the full dataset (*n* = 18 sites) and with a dataset excluding site T11, which underwent a large restoration in 2022-23 and therefore has an interrupted depositional history.

3.5.2 Regression of embeddedness by site

The same regression analyses were performed for site-averaged embeddedness as for volume. Embeddedness values (percentages) were averaged from approximately 55 samples per site and $\log_{10}$ transformed before regression was performed.

3.5.3 Regression of embeddedness by transect

Because embeddedness values and bedform were collected at individual transects, it is possible to regress transect-averaged embeddedness by bedform to test whether different bedforms are correlated with embeddedness. In this case, bedform is a fixed effect nested within site, a random effect. Bedforms included riffles, runs, pools, side channels, and backwaters. Riffles, runs, and pools are main channel bedforms, while side channels and backwaters describe off-channel bedforms (below bankfull). Because a transect can be classified as two bedforms (example: riffle with side channel), I created one dataset that included all transects (*n* = 213) and another with only main channel bedforms (*n* = 185) because geometric variables such as cross-sectional area and width-to-depth ratio are not comparable between main channel and off-channel settings.

To test the effect of bedform on embeddedness, I performed a mixed effect linear regression model with bedform as a fixed effect and site as a random effect using the *lmer* function from the lmerTest package (Kuznetsova et al., 2017). I then conducted an Anova test and pairwise comparisons between each bedform using Tukey-adjusted p-values. On the main channel dataset, I used *dredge* with a mixed model including bedform, site (random effect), reach location, cross-sectional area, and width-to-depth

ratio. Other reach-scale geometric variables like gradient and bank length ratio were not sampled at the transect level.

Table 2. Objectives and statistical tests used in multiple linear regression.

Objective & statisical tests	Formula	Reason	Notes
Volume by site			
lm, Anova, pairwise comparisons	Volume ~ reach location	does volume vary by reach location?	n = 18. skew right. Log_{10} transformation
Model selection - dredge	Volume ~ reach location + gradient + XSA + WDR + BLR	is distance downstream or site specific geometry more correlated with sediment volumes?	
Embeddedness by site			
lm, Anova, pairwise comparisons	Emb ~ reach location	does embeddedness vary by reach location?	n = 18. skew right. Log_{10} transformation
Model selection - dredge	Emb ~ reach location + gradient + XSA + WDR + BLR	is distance downstream or site specific geometry more correlated with embeddedness values?	
Embeddedness by transect			
lmer, Anova, pairwise comparisons	Emb ~ bedform + (1|site)	does embeddedness vary by bedform?	n = 213. normal distribution
Model selection - dredge	Emb ~ reach location + bedform + XSA + WDR	is distance downstream, bedform, or **transect** specific geometry more correlated with	main channel only. n = 185. normal distribution

3.1 Fine Sediment Mobilization and Flushing Flows

3.1.1 Flood recurrence intervals

To determine the flood recurrence intervals at the four modelling sites, I used available stream gauge data and, where these data were unavailable, regional estimates of flow recurrence from the US Geological Survey (USGS) StreamStats webpage (U.S. Geological Survey, 2019). The two transition zone sites are located near USGS stream gauges, each with over 40 years of continuous discharge readings, while the canyon sites do not have nearby gauges with continuous readings. There are several gauges within the canyon that have discontinuous records, but these are not conducive to determining flood recurrence intervals. The USGS gauges closest to Shields Street (Cache La Poudre River at Fort Collins, CO – 06752260) and to the Archery Range (Cache La Poudre River Above Boxelder Creek NR Timnath, CO – 06752280) have 48 and years of 44 years of continuous discharge readings, respectively. These gauges have sufficient records to capture the contemporary flow regime affected by widespread water withdrawals.

I downloaded peak flow data using the dataRetrieval package in R Statistical Software (De Cicco et al., 2018; United States Geological Survey, 1994) and ranked the peak flow from each year and determined the probability of occurrence over the given timespan and recurrence interval for each peak flow. I fit a logarithmic curve to the data and determined the 2-, 5-, and 10-year recurrence interval discharges for each stream gauge.

At the canyon sites (Pasquinels Cabin and Indian Meadows), no consistent record of streamflow exists for more than a decade, so I used USGS StreamStats to estimate the same recurrence interval discharges. StreamStats uses regional regression equations created for Colorado watersheds based on drainage area and elevation distribution within the watershed to estimate streamflow statistics. A stream gauge operated by the City of Fort Collins located just upstream of Indian Meadows (Fort Collins – Rustic) has streamflow records from prior to the Cameron Peak wildfire, and that gauge was used to determine the number of days the two canyon sites experienced each recurrence interval discharge.

To create hydrographs of the 2021 water year and compare streamflow throughout the mainstem Poudre River, I downloaded streamflow data from Colorado Division of Water Resources (Cache La Poudre at Canyon Mouth Near Fort Collins (CLAFTCCO)) and Larimer County (Fort Collins – Rustic – 11004, and Poudre River at Hewlett Gulch Bridge – 6770).

3.1.2 Sediment mobilization criteria

I determined bed sediment entrainment thresholds by calculating the critical shear stress for mobilizing the median diameter bed particle (D_{50}) at each site. The methods for bed mobilization are simplified due to the limited grain size data and project scope.

Bed (boundary) shear stress (τ_0) at a cross-section is calculated by $\tau_0 = \gamma RS$, where γ is the specific weight of water, *R* is the hydraulic radius (cross-sectional area divided by wetted perimeter; can be approximated as depth at wide cross sections), and *S* is water surface slope. The shear stress required to

mobilize a particle is the critical shear stress (τ_c). The Shields parameter (τ_*) is a dimensionless shear stress calculated by ratio of the bed shear stress to the weight of an immersed grain

$$\tau_* = \frac{\tau_0}{(\rho_s - \rho) g D_s} \quad \text{(equation 1)}$$

where ρ_s is the sediment density, ρ is the water density, g is the acceleration due to gravity, and D_s is grain size. Thus, the critical Shields parameter (τ_c^*) is defined by the ratio of critical shear stress to weight of an immersed grain

$$\tau_c^* = \frac{\tau_c}{(\rho_s - \rho) g D_s} \quad \text{(equation 2)}$$

where D_s is typically the median grain size. Shields (1936) empirically derived values for critical Shields parameter in flume studies with uniformly sized sand grains by plotting critical Shields parameter values against shear Reynolds number (Re_*) at the start of sediment mobilization. Values of the Shields parameter generally vary between 0.03 and 0.08, but at high Re_* (larger grain size), the value reaches a constant of approximately 0.047, or it can be approximated by $\tau_c^* \cong 0.06 tan\phi$ when $Re_* > 50$ (ϕ is the angle of repose) (Julien, 2010). In this study, I use the τ_c^* values listed in Table 7.1 from Julien (2010).

In gravel-bed rivers with sediment mixtures, a coarse-grained armor layer, or pavement, typically forms on the bed surface as low to moderate flows remove the finer portion of the sediment at the surface (Parker & Klingeman, 1982; Parker & Toro-Escobar, 2002). The remaining fine sediment becomes shielded by the coarse armor layer and will only mobilize if the coarse grains mobilize. The concept of equal mobility states that all fractions of the sediment mixture are transported at the same rate (Church et al., 1991; Parker & Klingeman, 1982). In other words, the armor layer must be mobilized for the underlying fine material to mobilize (Julien, 2010). Wilcock (1993) concluded that individual fractions in a range of unimodal sediment size distributions begin to move at nearly the same flow strength because the critical shear stress of smaller grains is increased due to reduced flow exposure, while the opposite is

true for coarser grains. Therefore, the critical shear stress of the D_{50} of a mixture is commonly used to estimate the entrainment of the whole bed (Julien, 2010; Wilcock et al., 2009). In an entrainment study of gravel-bed rivers in the Rocky Mountain region of Colorado, Andrews (1984) found that bankfull shear stress exceeded the threshold value for entrainment of the median particle diameter of the bed surface and resulted in the entrainment of the majority of the bed material.

Other research has suggested that mobilization of grains is selective and that the critical shear stress for certain particle sizes depends on their size relative to the rest of the bed (D_i/D_{50}) (Komar, 1987; Powell, 1998). Although there are methods for determining critical shear stress values for portions of sediment mixtures, the sediment size sampling protocol used here does not yield the proper grain-size distribution needed for such methods. Here I assume the principle of equal mobility and use median grain size to determine the critical shear stress and assume that bed mobilization occurs at that critical shear stress.

At sites sampled for this study, the high embeddedness values indicate the interstitial space between grains in the coarse armor layer is filled in with fines. Of the many objectives of flushing flows, Kondolf & Wilcock (1996) specify that mobilizing gravel is necessary to restore and enhance riffle habitat by removing interstitial fines. I assume that the coarse grains must mobilize to flush the fines from the interstitial spaces within the armor layer.

3.1.3 Hydraulic modelling

Two-dimensional hydraulic modelling was performed using the Hydraulic Engineering Center-River Analysis System (HEC-RAS) version 6.4.1 (US Army Corps of Engineers, 2023). Terrain surfaces used in hydraulic modelling are described in sections 3.4.3 and 3.4.4. Although some elevation error occurred as a result of refraction through the water surface during the SfM DEM creation, calibration of the hydraulic models to known water surface elevations was successful, and I concluded that the errors

were acceptable for the purpose of the modelling. Manning's *n* roughness values were calibrated at low flows to water-surface elevations during the time of RTK and drone surveys. At canyon sites (Pasquinels Cabin and Indian Meadows), where the terrain surface was created from RTK points, I calibrated the flow during the time of surveys to surveyed water surface elevations in the vertical dimension and to the wetted boundary in the horizontal dimension using the Rustic stream gauge. At transition zone sites (Shields Street and Archery Range), where the terrain surface was created from SfM, I calibrated the flow during the time of surveys to water surface elevations in the vertical dimension and to the wetted boundary in the horizontal dimension by using the orthophoto. At Shields Street, I measured discharge because the nearest gauge (USGS 06752260 – Fort Collins) is 4 km downstream and may not accurately represent the flow at the site, and at the Archery Range, I used the Timnath gauge (USGS 06752280), which is only 1 km upstream. I also used a Google Earth image from June 2022 to calibrate the model parameters at a moderately high flow of 30 m^3/s.

For Pasquinels Cabin and Indian Meadows, the channel computational cells were 2 m by 2 m, and the floodplain cells were 4 m by 4 m. I ran an unsteady flow model with a stepped hydrograph using the 2-, 5-, and 10-year recurrence interval discharges and a 1-second computational interval to keep the Courant numbers below 5. The maximum Courant numbers were 3.4 and 2.4 for Pasquinels Cabin and Indian Meadows, respectively. For Shields Street and the Archery Range, channel computational cells were 1 m by 1 m with 4 m by 4 m floodplain cells, and I used a 0.5 second computational interval to keep Courant numbers below 2.8 and 2.4, respectively.

In RAS Mapper, I added a shear stress output in Pascals from each step of the hydrograph and exported them as raster files. In QGIS, I used the raster calculator to convert the original raster file into dimensionless shear stress units and filtered values greater than or equal to the dimensionless critical shear stress at each site to show what portion of the bed is likely experiencing mobilization. I used the

Raster Layer Zonal Statistics tool to quantify the area of each raster and divided that area by the channel area to calculate the proportion of channel above critical shear stress.

4. RESULTS

4.1 Sediment Retention

I present results from individual regression and model selection of multiple linear regression models here. Both sediment retention variables are tested against site-averaged variables and watershed-scale variables, and embeddedness is also tested against transect-level geometry in a mixed model. A summary of site data is presented in Table 3.

For both sediment retention metrics, model selection indicates that reach location is a better predictor than reach scale variables, but some reach scale variables are significant indicators. Gradient and bank length ratio have some explanatory power for volume, and gradient and cross-sectional area have explanatory power for embeddedness. At the transect level, pools have the highest embeddedness of main channel bedforms, and side channels have a wide range of values. All backwaters are 100% embedded.

Table 3. Data summary for all sites. Emb: embeddedness. Dashed line separates canyon sites up and downstream of Black Hollow and between canyon and transition zone sites. "Control" indicates upstream of Black Hollow. Asterisks indicate modelling sites.

	Fine sediment retention			Distance downstream		Site-specific variables				
Site	Fine sediment volume (m^3)	Fine sediment volume per bankfull volume (m^3/m^3)	Emb (%)	Dist DS from BH (km)	Reach location	Gradient (bed) (m/m)	Gradient (water surf.) (m/m)	Cross-sectional area (m^2)	Width-to-depth ratio (m/m)	Bank length ratio (m/m)
Bliss	232	0.0259	56.4	-10.0	control	0.0032	0.0024	31.4	39.1	3.12
Pasquinels*	52	0.0062	55.5	-5.0	control	0.0050	0.0028	28.5	36.2	2.06
Black Hollow	70	0.0115	52.5	-0.6	control	0.0111	0.0133	21.6	33.2	2.07
Fire Lane	133	0.0194	43.5	1.8	canyon	0.0100	0.0128	23.5	30.6	2.01
Indian Meadows*	128	0.0167	54.1	12.9	canyon	0.0086	0.0086	24.9	39.6	2.93
Kelley Flats	59	0.0063	43.3	16.6	canyon	0.0076	0.0086	31.1	42.5	3.22
Dutch George	77	0.0088	37.3	23.0	canyon	0.0092	0.0102	27.3	67.1	3.22
Stove Prairie	21	0.0025	42.8	31.6	canyon	0.0098	0.0097	28.6	31.0	2.01
Hewlett Gulch	66	0.0085	45.0	41.8	canyon	0.0055	0.0086	25.6	51.5	2.23
Gateway	5	0.0008	30.5	51.0	canyon	0.0070	0.0094	20.8	20.8	2.00
Lions Park	100	0.0123	53.8	68.7	transition	0.0068	0.0062	28.7	34.6	3.25
T03 (Shields St.)*	100	0.0136	61.3	73.7	transition	0.0059	0.0054	22.6	30.1	2.04
T04	367	0.0412	58.0	75.0	transition	0.0016	0.0026	30.8	30.9	2.10
T06	886	0.1376	56.8	77.5	transition	0.0013	0.0024	19.9	21.7	2.65
T08	521	0.0525	56.0	80.6	transition	0.0052	0.0025	27.4	24.8	2.48
T10	362	0.0514	88.1	84.0	transition	0.0017	0.0012	32.6	23.9	2.50
T11	394	0.0445	48.0	84.5	transition	0.0058	0.0062	33.9	53.0	3.03
T12 (Archery Range)*	592	0.0475	71.5	86.9	transition	0.0012	0.0016	42.0	22.5	2.87

4.1.1 Fine sediment volumes by site

Bivariate plots of site-averaged geometric attributes indicate that gradient is the only significant individual predictor of fine sediment volume (R^2 = 0.37, p = 0.008; Figure 9A). Gradient has a negative correlation with volume, which is expected. Average cross-sectional area, average width-to-depth ratio, and bank length ratio show weak explanatory power individually.

Two trends are noticeable from the plot of volume against distance downstream (Figure 9B). First, fine sediment volumes decrease with increasing distance downstream until the transition zone, where they increase rapidly. Second, reach location has a statistically significant effect on volume (Anova; p = 0.005; Figure 9C). In Figure 10, pairwise comparisons of estimated means indicate that transition zone sites have significantly higher fine sediment volumes than canyon reaches downstream of Black Hollow (p = 0.004). Sites upstream of Black Hollow do not have statistically significant different levels of fine sediment relative to either canyon sites downstream of Black Hollow or transition zone sites (p = 0.53 and p = 0.18, respectively). There are only three sites upstream of Black Hollow, so the small sample size may not adequately represent the whole region.

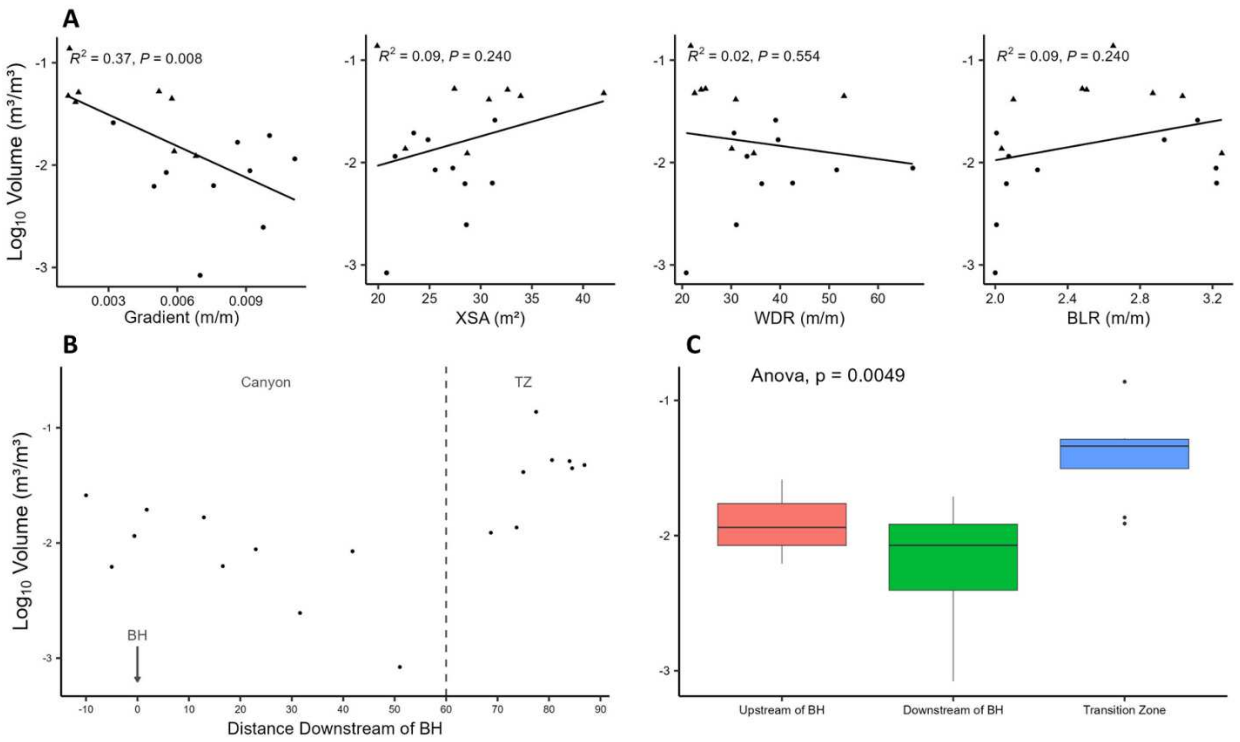

Figure 9: (A) Bivariate plots of log_{10}(volume) versus reach scale variables. (B) log_{10}(volume) versus distance downstream (C) log_{10}(volume) versus reach location. XSA: cross-sectional area; WDR: width-to-depth ratio; BLR: bank length ratio; BH: Black Hollow creek confluence; TZ: Transition zone.

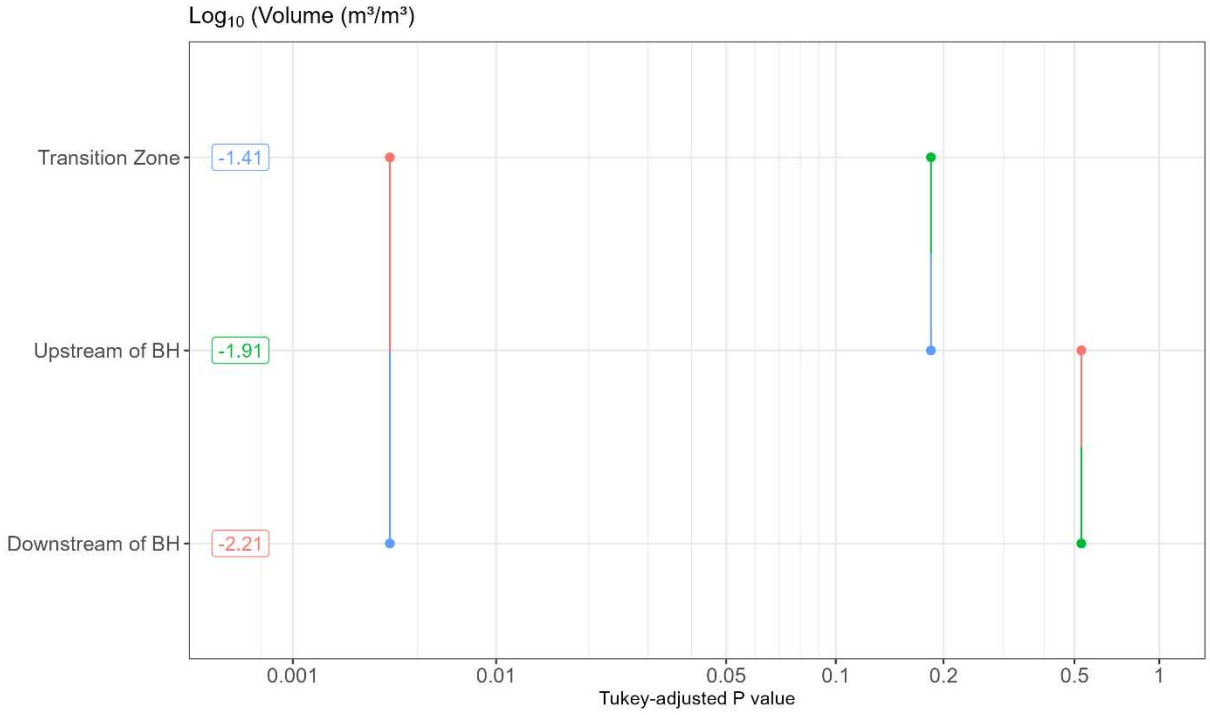

Figure 10. Pairwise comparisons of estimated means with Tukey-adjusted P values of log_{10}(volume) by reach location.

Model selection of the full dataset and dataset with site T11, which is removed because of the recent restoration project, yield two models each that are considered to have substantial support with a Delta AICc of 2 or less (Table 4). Site T11 was restored and had major channel reconfigurations in 2022, so the site doesn't record the same depositional history as the others. The best predictors of fine sediment volume were gradient and a categorical indicator of distance downstream for both datasets, but the order was reversed; the distance downstream predictor is the strongest for the full dataset, and gradient is the strongest for the reduced dataset.

For both datasets, bank length ratio (BLR) is the next most substantial predictor and barely falls out of the threshold of 2 Delta AICc (Delta AICc = 2.10 for full, 2.58 for reduced). I investigate the potential significance of this variable in the Discussion.

Table 4. Top ten models predicting log_{10}(volume) from dredge output of full dataset and one without site T11. Models with Delta AICc ≤ 2 were considered to have substantial support and are bolded. location: reach location; grad_bed: gradient; BLR: bank length ratio; WDR_ave: width-to-depth ratio; XSA_ave: cross-sectional area

Log_{10}(volume) - full dataset

Model	df	AICc	Delta AICc	AICc Weight	Log likelihood
location	**4**	**25.78**	**0.00**	**0.30**	**-7.35**
grad_bed	**3**	**26.94**	**1.16**	**0.17**	**-9.61**
BLR + location	5	27.88	2.10	0.10	-6.44
location + grad_bed	5	28.66	2.88	0.07	-6.83
BLR + grad_bed	4	28.86	3.08	0.06	-8.89
location + WDR_ave	5	28.95	3.17	0.06	-6.97
location + XSA_ave	5	29.57	3.79	0.04	-7.29
grad_bed + WDR_ave	4	30.13	4.36	0.03	-9.53
grad_bed + XSA_ave	4	30.29	4.51	0.03	-9.61
BLR + location + grad_bed	6	31.55	5.77	0.02	-5.96

Log_{10}(volume) - no T11

Model	df	AICc	Delta AICc	AICc Weight	Log likelihood
grad_bed	**3**	**25.81**	**0.00**	**0.28**	**-8.98**
location	**4**	**26.16**	**0.36**	**0.23**	**-7.42**
BLR + grad_bed	4	28.38	2.58	0.08	-8.53
BLR + location	5	28.57	2.76	0.07	-6.56
location + grad_bed	5	29.15	3.35	0.05	-6.85
grad_bed + XSA_ave	4	29.25	3.44	0.05	-8.96
grad_bed + WDR_ave	4	29.29	3.49	0.05	-8.98
location + WDR_ave	5	29.49	3.68	0.04	-7.02
location + XSA_ave	5	30.18	4.37	0.03	-7.36
intercept - only model	2	31.00	5.19	0.02	-13.07

4.1.2 Embeddedness by site

Bivariate plots of log_{10}(embeddedness) show better correlation of individual reach-scale variables (Figure 11A). Gradient is, again, the strongest predictor of embeddedness (p = 0.005), whereas cross-sectional area shows moderate explanatory power (p = 0.067). Embeddedness is negatively correlated with gradient and positively correlated with cross-sectional area, indicating high sediment deposition in

low gradient, low velocity reaches. Width-to-depth ratio and bank length ratio show less explanatory power (p = 0.115 and p = 0.76, respectively).

Embeddedness levels follow a similar trend to volumes when plotted against distance downstream, with decreasing values throughout the canyon and increasing values in the transition zone (Figure 11B). Reach location has a statistically significant effect on embeddedness (Anova Type II test; p = 0.003; Figure 11C). In Figure 12, pairwise comparisons of estimated means indicate that transition zone sites have significantly higher embeddedness than canyon reaches downstream of Black Hollow (p = 0.002). Sites upstream of Black Hollow have greater levels of fine sediment than canyon sites downstream of Black Hollow, but it is only significant at an alpha of 0.1 (p = 0.09). Sites upstream of Black Hollow do not have a statistically significant difference in embeddedness relative to transition zone sites (p = 0.66).

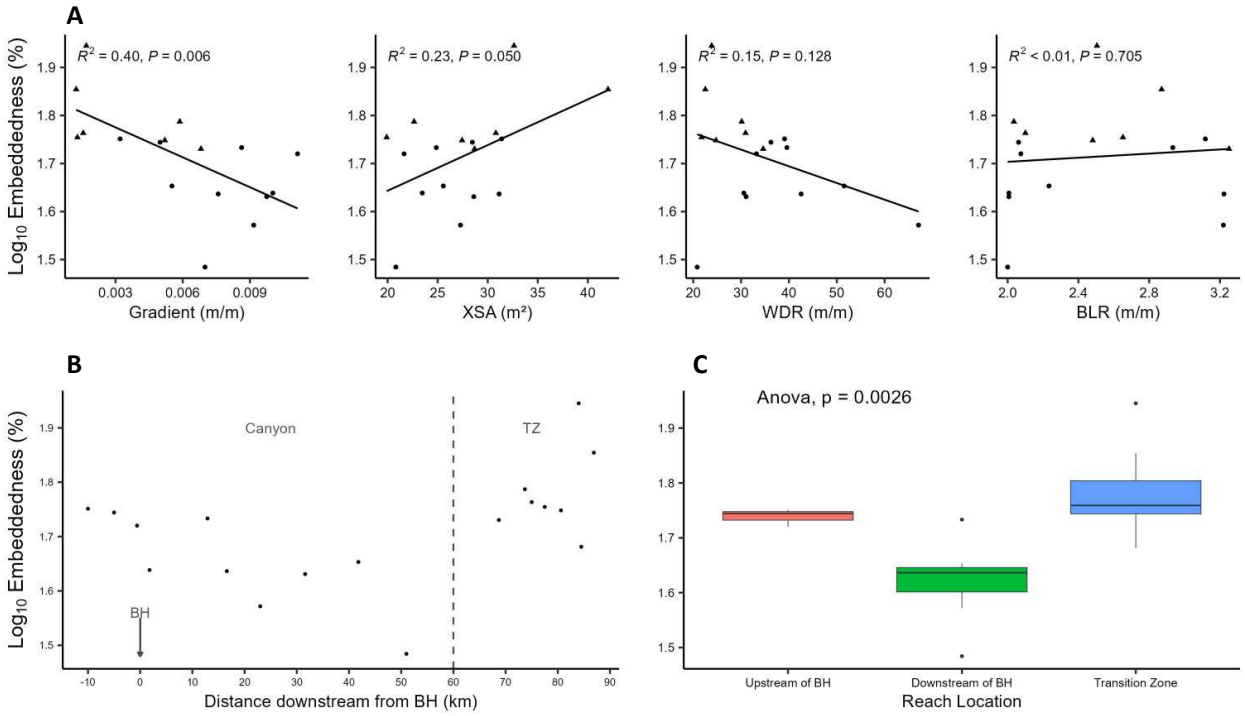

Figure 11: (A) Bivariate plots of log10(embeddedness) versus reach scale variables. (B) log10(embeddedness) versus distance downstream. (C) log10(embeddedness) versus reach location. XSA: cross-sectional area; WDR: width-to-depth ratio; BLR: bank length ratio; BH: Black Hollow creek confluence; TZ: Transition zone

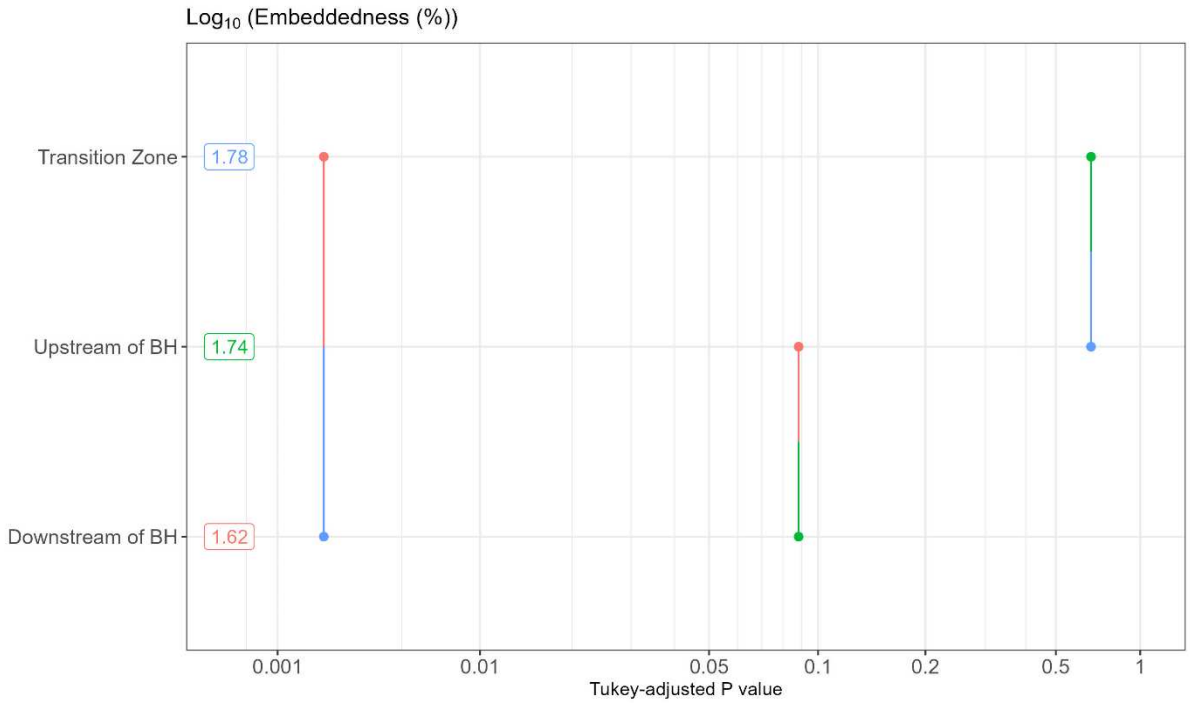

Figure 12. Pairwise comparisons of estimated means using Tukey-adjusted P values of embeddedness by reach location

Model selection for predictors of embeddedness of the full dataset and dataset with site T11 removed yield three or two models considered to have substantial support with a Delta AICc of 2 or less, respectively (Table 5). For the full dataset, the best model was embeddedness as a function of reach location, followed by a model with gradient as the sole predictor (Delta AICc = 1.71). The next best supported model had reach location and cross-sectional area as predictors. For the dataset without site T11, the top model had reach location as the sole predictor, followed by one with reach location and cross-sectional area (Delta AICc = 0.25).

Table 5. Top ten models predicting embeddedness from dredge output for full dataset and one without site T11. Models with Delta AICc ≤ 2 were considered to have substantial support and are bolded. location: reach location; grad_bed: gradient; BLR: bank length ratio; WDR_ave: width-to-depth ratio; XSA_ave: cross-sectional area

Log_{10} (Embeddedness) - full dataset

Model	df	AICc	Delta AICc	AICc Weight	Log likelihood
location	**4**	**-34.71**	**0**	**0.30**	**22.89**
grad_bed	**3**	**-33.00**	**1.71**	**0.13**	**20.36**
location + XSA_ave	**5**	**-32.85**	**1.86**	**0.12**	**23.93**
grad_bed + location	5	-32.48	2.23	0.10	23.74
location + WDR_ave	5	-31.29	3.42	0.05	23.14
BLR + location	5	-30.80	3.90	0.04	22.90
grad_bed + XSA_ave	4	-30.60	4.11	0.04	20.84
grad + WDR_ave	4	-30.47	4.23	0.04	20.77
BLR + grad_bed	4	-29.64	5.07	0.02	20.36
location + WDR_ave + XSA_ave	6	-29.60	5.11	0.02	24.62

Log_{10}(Embeddedness) - no T11

Model	df	AICc	Delta AICc	AICc Weight	Log likelihood
location	**4**	**-33.56**	**0**	**0.33**	**22.45**
location + XSA_ave	**5**	**-33.30**	**0.25**	**0.29**	**24.38**
grad_bed + location	5	-30.41	3.15	0.07	22.93
grad_bed	3	-29.83	3.73	0.05	18.84
BLR + location	5	-29.73	3.83	0.05	22.59
location + WDR_ave	5	-29.46	4.09	0.04	22.46
grad_bed + location + XSA_ave	6	-28.45	5.11	0.03	24.43
BLR + location + XSA_ave	6	-28.43	5.12	0.03	24.42
location + WDR_ave + XSA_ave	6	-28.39	5.17	0.02	24.39
grad_bed + XSA_ave	4	-27.69	5.87	0.02	19.51

4.1.3 Embeddedness by transect

Embeddedness varies by bedform when analyzed by transect in a mixed model with site as a random effect (Anova, $p < 0.001$; Figure 13). Of main channel bedforms, riffles have the lowest embeddedness values, and embeddedness values increase in runs and pools, which represent lower energy environments. Both off-channel bedforms have higher embeddedness values than the main channel bedforms. Side channels have the widest range of values, and all backwaters are 100% embedded. Backwaters only occurred in the transition zone and were associated with former channels or the mouths of side channels.

Pairwise comparisons of all bedforms using Tukey-adjusted P values, indicate that all bedforms have statistically significant differences in embeddedness, except for three scenarios: between pools and backwaters, side channels and backwaters, and pools and side channels (Figure 14; $p = 0.09$, 0.24, & 0.97, respectively). This indicates that off-channel areas and low-energy environments within the main channel preferentially accumulate fine sediment.

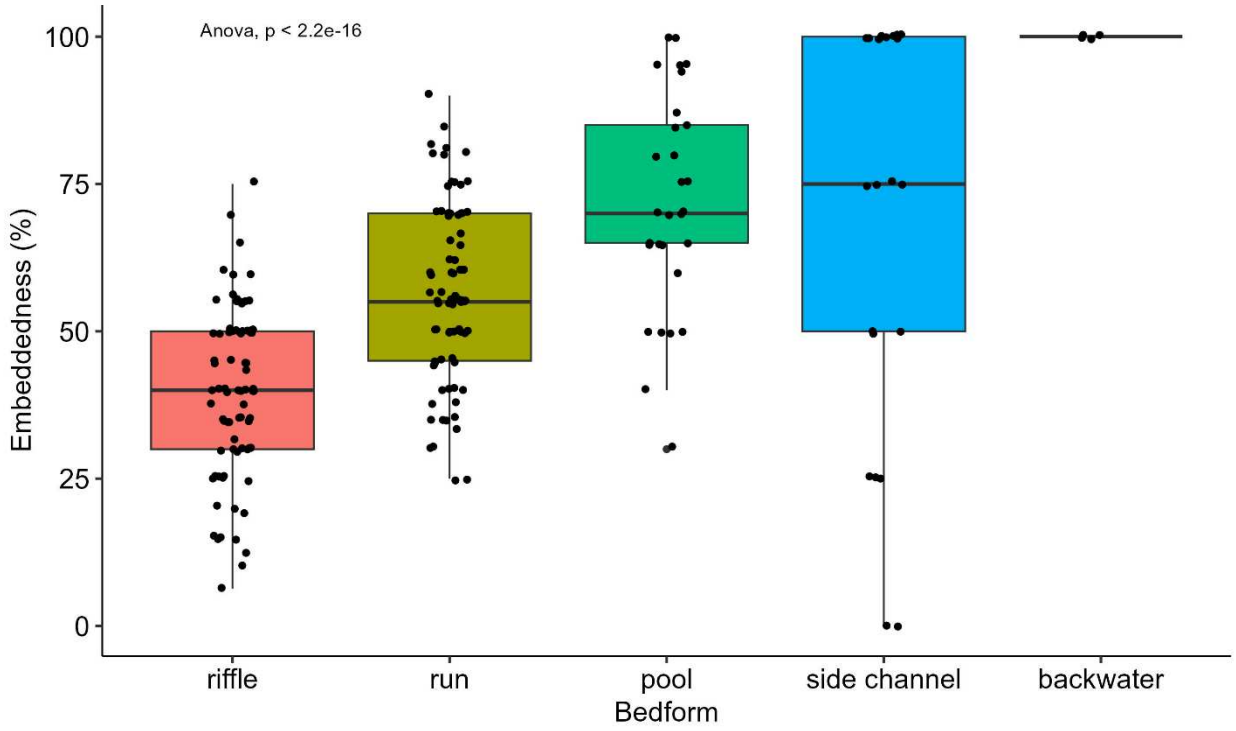

Figure 13. Box plot of embeddedness versus bedform. Horizontal line indicates median, box indicates interquartile range, vertical line is the range, and each point is an averaged transect.

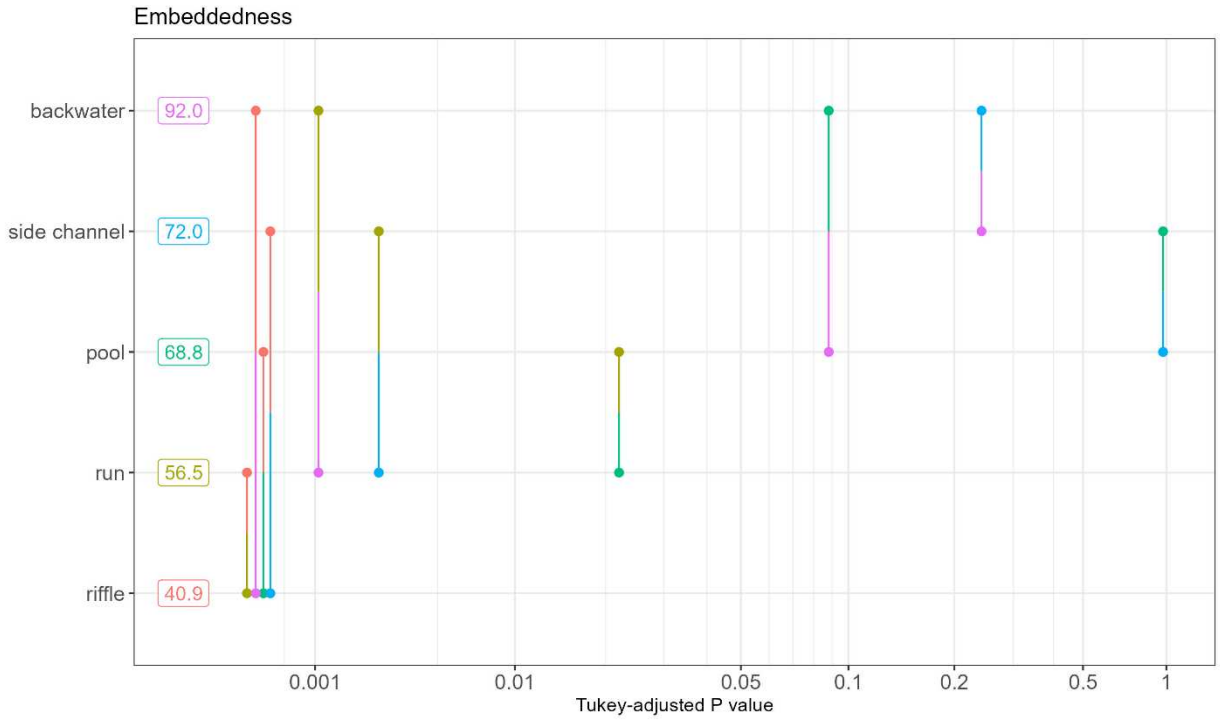

Figure 14. Tukey-adjusted P values of embeddedness by bedform.

Model selection of embeddedness of main channel bedforms with reach-scale variables yields three substantially supported models (Table 6). The highest has bedform as a single predictor, the next highest has bedform and cross-sectional area (Delta AICc = 1.1), and the next highest has bedform and width-to-depth ratio as predictors (Delta AICc = 1.9). Cross-sectional area and width-to-depth ratio both have positive correlation with embeddedness.

Table 6. Top ten models predicting embeddedness by transect from dredge() output for main channel transects (not including side channels or backwaters). Models with Delta AICc ≤ 2 were considered to have substantial support and are bolded. WDR_ave: width-to-depth ratio; XSA_ave: cross-sectional area.

Embeddedness by Transect - main channel

Model	df	AICc	Delta AICc	AICc Weight	Log likelihood
bedform	**5**	**1503.4**	**0**	**0.46**	**-746.71**
bedform + XSA	**6**	**1504.5**	**1.1**	**0.27**	**-746.25**
bedform + WDR	**6**	**1505.4**	**1.9**	**0.17**	**-746.68**
bedform + WDR + XSA	7	1506.5	3.1	0.10	-746.24
WDR	4	1583.5	80.1	0.00	-787.77
WDR + XSA	5	1583.7	80.3	0.00	-786.84
intercept model	3	1584.1	80.7	0.00	-789.05
XSA	4	1585.0	81.6	0.00	-788.51

4.2 Fine Sediment Mobilization and Flushing Flows

Figure 15 displays DEMs of each hydraulic modelling site with elevations relative to the lowest elevation in each site. Table 7 and Figure 16 show the proportion of the channel above the threshold critical shear stress at the 2-, 5-, and 10-year recurrence interval flow for each site, and Figures 17-20 show the detailed dimensionless shear stress outputs at each site. Since the Cameron Peak wildfire, Pasquinels Cabin and Indian Meadows have experienced 14 days with flows at or above the 2-year flow, compared to 6.8 and 3.7 days for Shields Street and the Archery Range. The two canyon sites have experienced 1 day at the 5-year flow level, and Indian Meadows experienced 0.2 days at the 10-year flow level, which was during the Black Hollow debris flow (the gauge used here is between Pasquinels Cabin and Indian Meadows and downstream of Black Hollow, so Pasquinels Cabin would not have experienced that high flow event). Neither transition zone site experienced a 5- or 10-year flow event. The difference between canyon and transition zone flows may be a result of flow alteration due to water withdrawals during spring runoff.

Indian Meadows likely experiences the most bed mobilization (31%) during the 2-year flow, while all other sites experience negligible bed mobilization. At the 5-year flow, Shields Street experiences a sharp jump to 36% of the channel, while the Archery Range is only 13%. Likewise, the 10-year flow shows that at Indian Meadows and Shields Street over 50% of the channel experiences bed mobilization, while the Archery Range shows 16%. The results from modelling show very little substrate mobilization at Pasquinels Cabin at all discharges. These results indicate that bed mobilization occurs at different rates in the study area and validates the finding that reach location (canyon versus transition zone) is correlated with fine sediment retention.

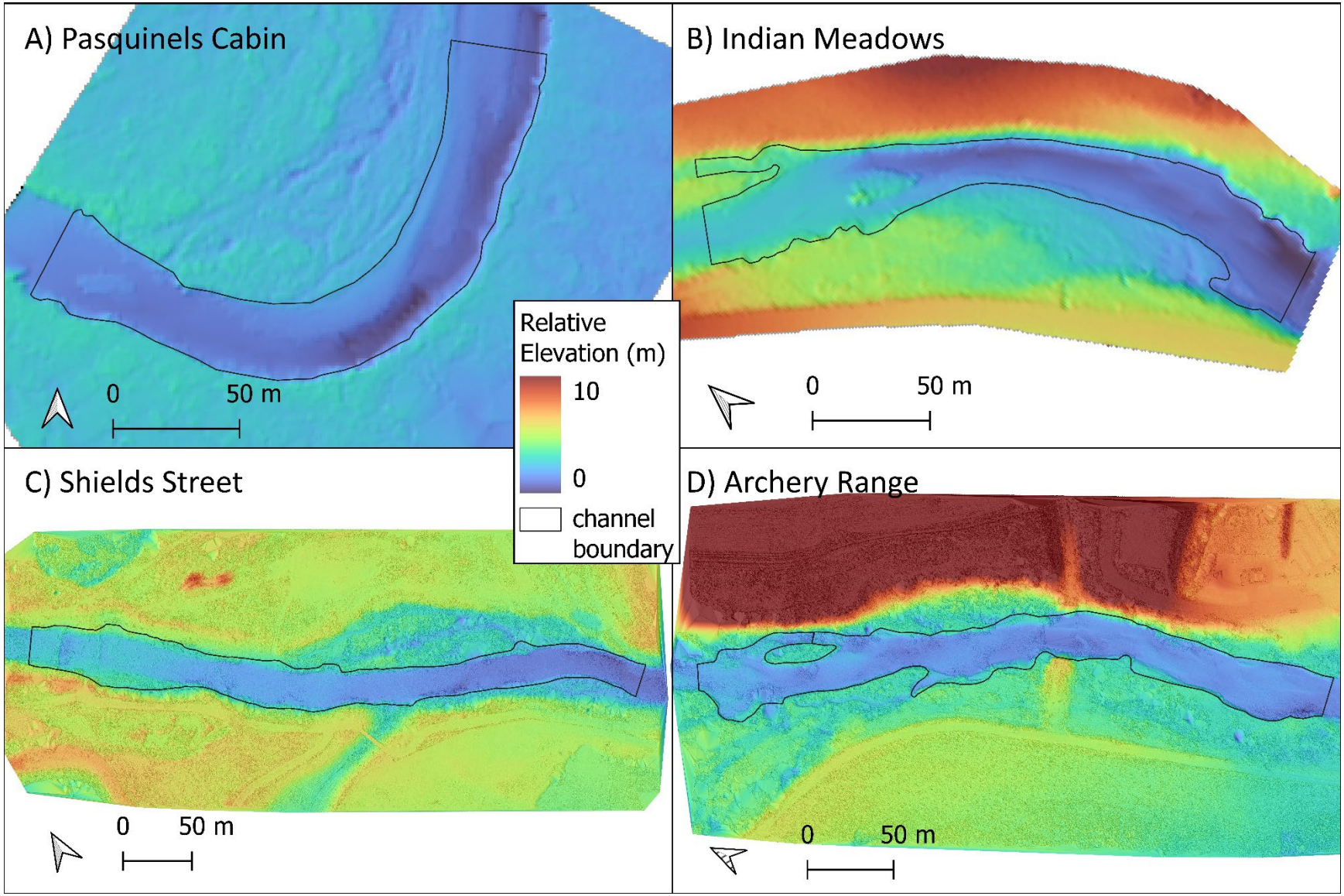

Figure 15. Digital elevation models of hydraulic modelling sites overlain onto hillshade images. Elevations are relative to the minimum elevation of each site. Flow is from left to right in each panel.

Table 7. Hydraulic modelling site summaries. RI: recurrence interval; Emb: embeddedness; Q: discharge; CPF: Cameron Peak wildfire

Site	Slope (m/m)	D50 (mm)	Emb. (%)	RI (years)	Q (m^3/s)	Q (ft^3/s)	n. days ≥ Q since CPF	τ_c* (-)	τ_c (Pa)	Proportion of channel ≥ τ_c (%)
Pasquinels Cabin	0.005	43	56	2	37	1307	14	0.052	36	0%
				5	51	1801	1			1%
				10	61	2154	0			4%
Indian Meadows	0.009	107	54	2	37	1307	14	0.054	96	31%
				5	51	1801	1			50%
				10	61	2154	0.2			59%
Shields Street	0.006	65	61	2	60	2119	6.8	0.05	56	1%
				5	112	3955	0			36%
				10	151	5333	0			54%
Archery Range	0.001	43	72	2	54	1907	3.7	0.052	36	3%
				5	105	3708	0			13%
				10	143	5050	0			20%

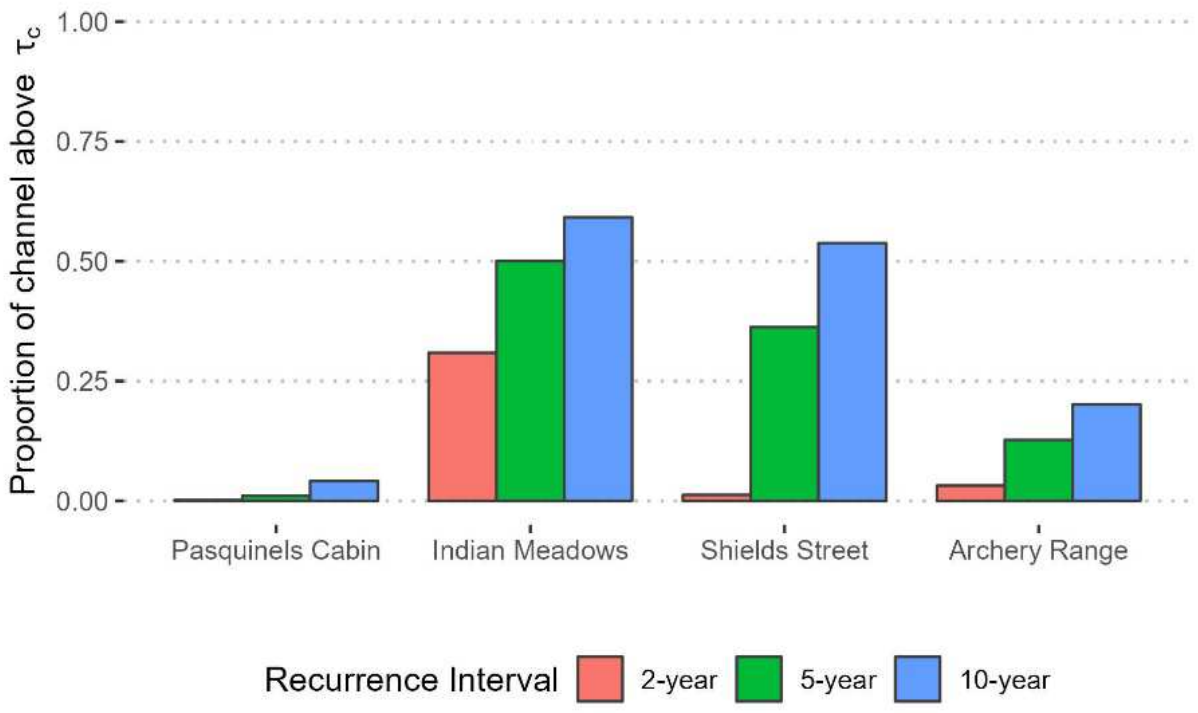

Figure 16. Hydraulic modelling results showing proportion of channel above τ_c for each recurrence interval flow at each site.

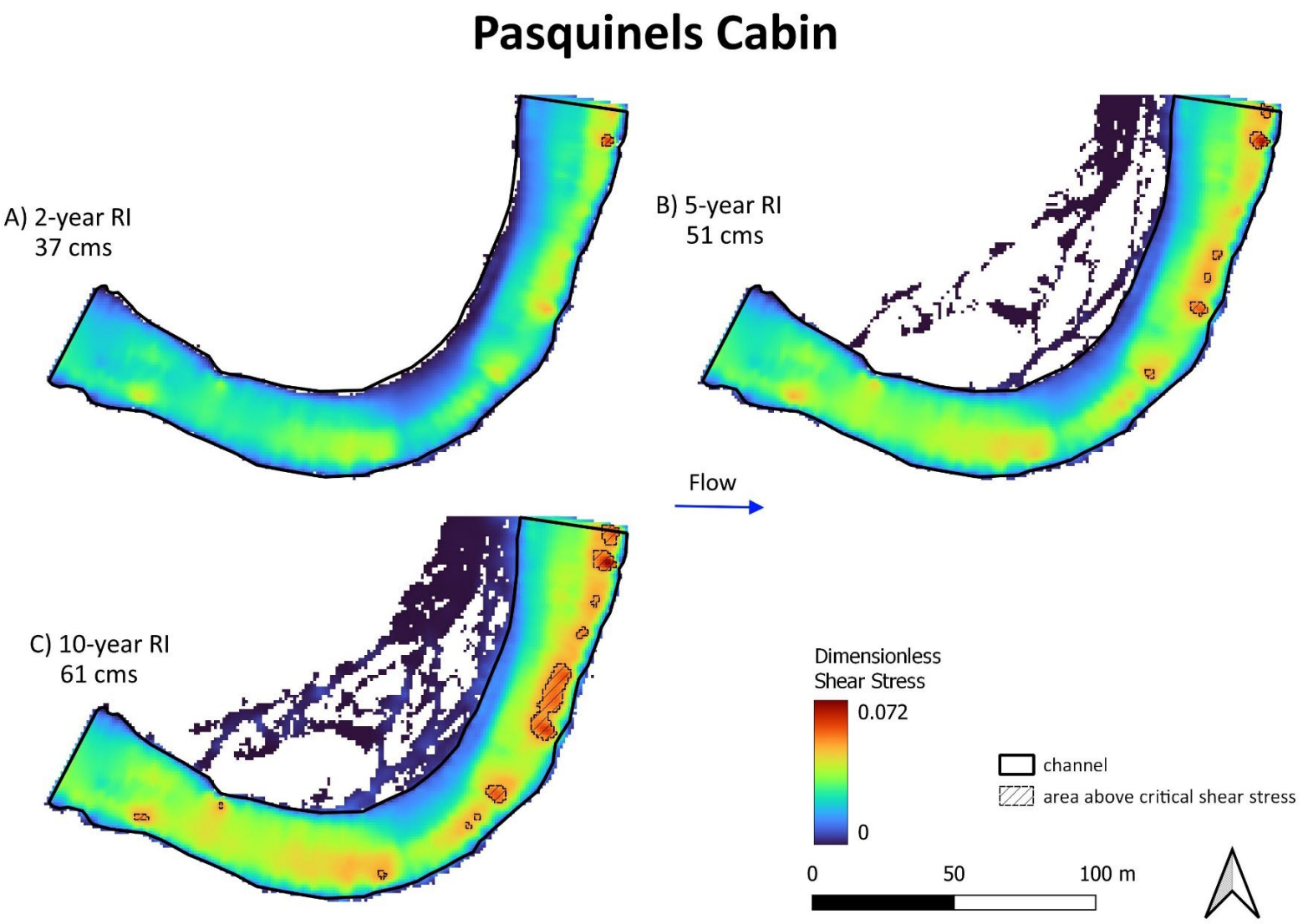

Figure 17. Bed mobilization potential at Pasquinels Cabin. (A), (B), and (C) show dimensionless shear stress outputs at 2-, 5-, and 10-year recurrence interval flows. Shaded areas are where bed shear stress is greater than critical shear stress, indicating bed mobilization. Blue arrow indicates flow direction.

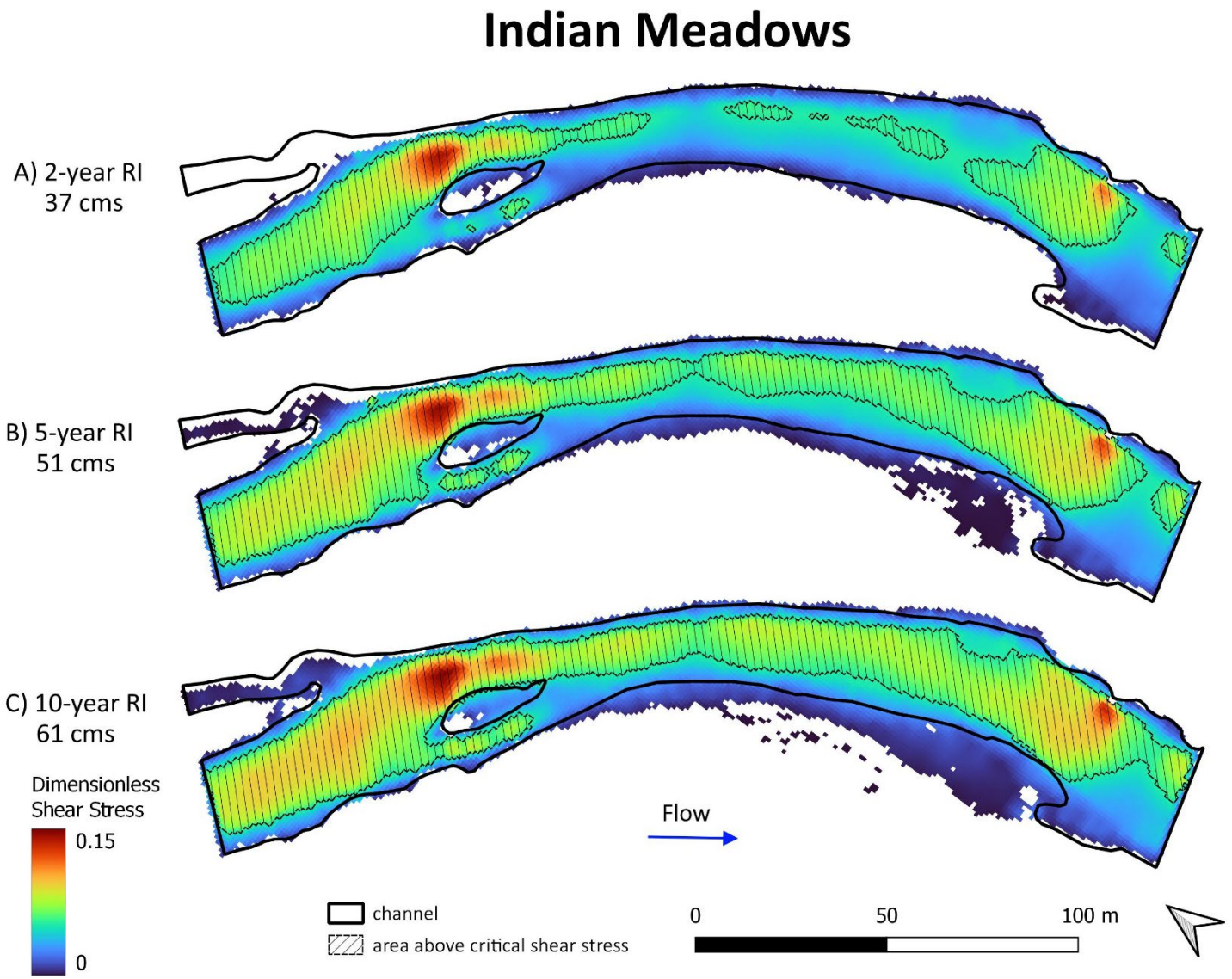

Figure 18. Bed mobilization potential at Indian Meadows. (A), (B), and (C) show dimensionless shear stress outputs at 2-, 5-, and 10-year recurrence interval flows. Shaded areas are where bed shear stress is greater than critical shear stress, indicating bed mobilization. Blue arrow indicates flow direction.

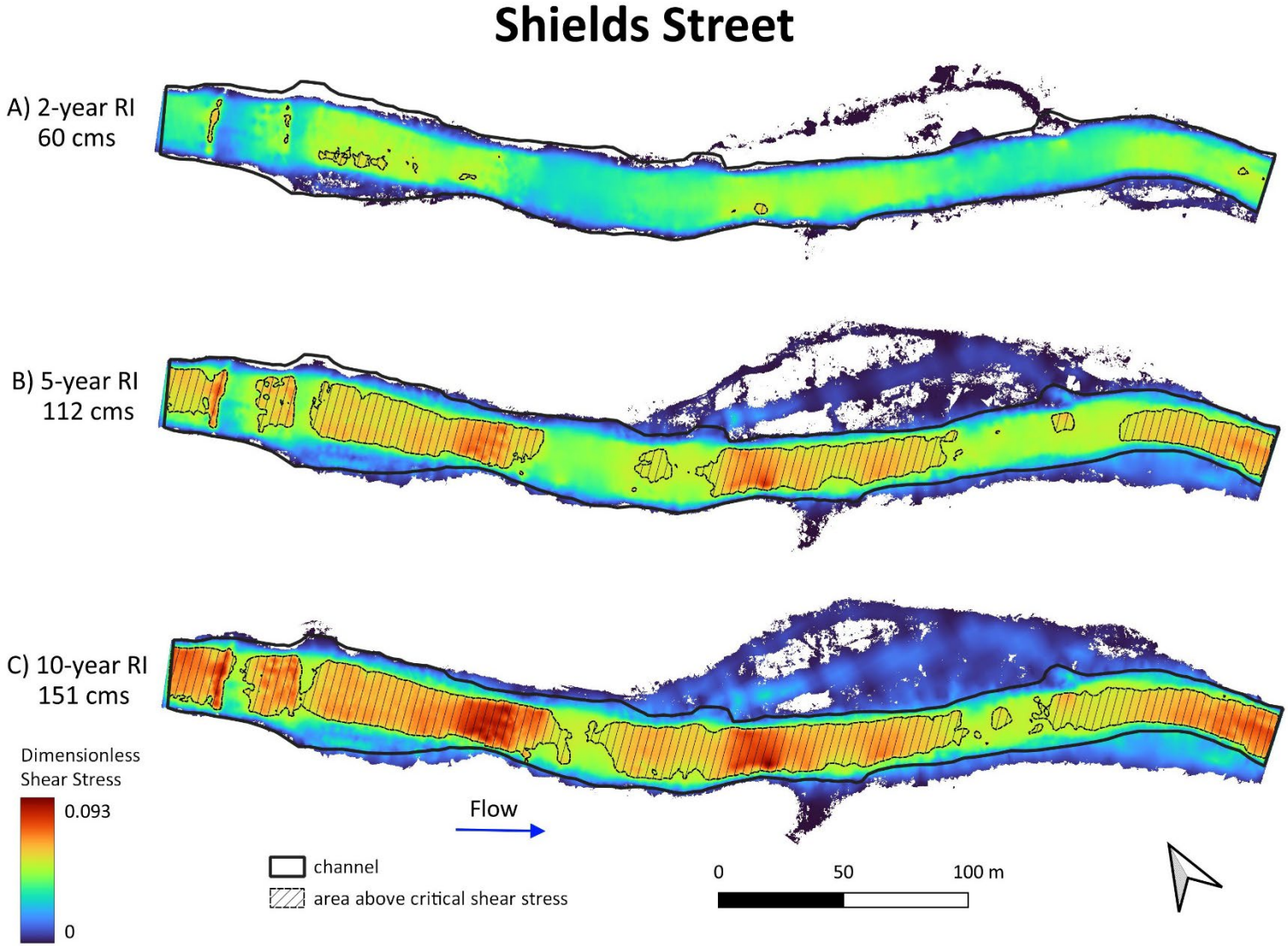

Figure 19. Bed mobilization potential at Shields Street. (A), (B), and (C) show dimensionless shear stress outputs at 2-, 5-, and 10-year recurrence interval flows. Shaded areas are where bed shear stress is greater than critical shear stress, indicating bed mobilization. Blue arrow indicates flow direction.

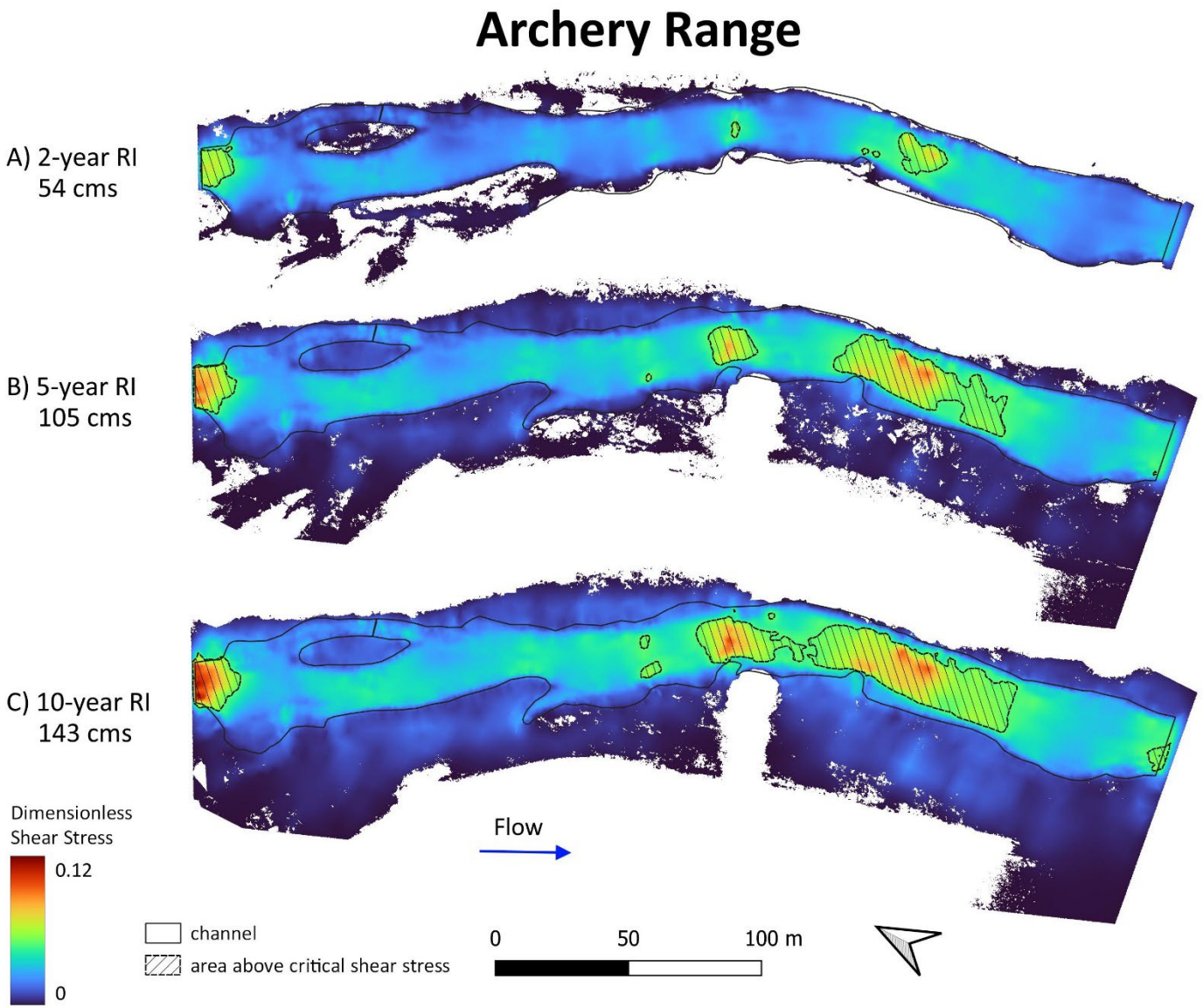

Figure 20. Bed mobilization potential at Archery Range. (A), (B), and (C) show dimensionless shear stress outputs at 2-, 5-, and 10-year recurrence interval flows. Shaded areas are where bed shear stress is greater than critical shear stress, indicating bed mobilization. Blue arrow indicates flow direction.

5.1 Fine Sediment Volumes

Multiple linear regression models that include bank length ratio as a predictor of reach-averaged deposit volumes fall slightly outside of the threshold of 2 Delta AIC_c units for substantially supported models, but better than the "considerably less" level of empirical support (Table 8; Burnham & Anderson, 2002). Although bank length ratio does not show explanatory power individually, I noticed the largest deposits in backwaters and marginal eddies where bank length is greater. This is not reflected in the statistical models perhaps because these features are small relative to the size of the site. Regardless of the statistical significance, the impact to habitat is concentrated in marginal eddies, side channels, and backwaters, where bank length is greater, and deposition in these areas may have an outsized effect on the aquatic ecosystem.

Table 8. Levels of empirical support for models based on Delta AIC. From Burnham and Anderson (2002)

Δ_i	Level of Empirical Support of Model i
0-2	Substantial
4-7	Considerably less
> 10	Essentially none.

I interpret deposits in marginal eddies as being caused by flow separation and recirculating flow during high and moderate flows. Fine sediment deposition patterns in large rivers may be analogous to those in the Poudre River. For example, on the Colorado River in the Grand Canyon, marginal sand bars form from recirculating eddies downstream of constrictions caused by debris fans at tributaries (Schmidt, 1990). Page & Nanson (1982) describe fine-grained marginal deposition associated with flow separation at concave banks (cut-banks) upstream of sharp meander bends. These deposits begin as isolated benches that, over time, are vegetated as trees establish. These deposits become part of the floodplain through lateral accretion, a process that is distinctly different from the more familiar lateral point-bar accretion.

After a reservoir sediment release on the North Fork Poudre of silt-to gravel-sized sediment, fine-grained deposition occurred in pools, and subsequent high flows scoured the fines in the center of the pools but did not completely remove deposits in the margins (Wohl & Cenderelli, 2000). The presence of some marginal deposits surveyed in my study three years after the fire leads me to believe that, without a major flood, some of them may become vegetated, stabilized, and accreted to the bank. This could lead to changes in erosion and deposition patterns in the future.

Large accumulations of fine sediment in backwaters and side channels, which occurred primarily in the transition zone, reflect similar low-energy areas that likely remain depositional during high flows. At sites T06, T08, T10, and T12, deposition in and around backwaters and side channels reduces habitat size and connection to the main channel (Figures 21 and 22). These intermittently connected off-channel habitats may act as source populations for rare native fishes including northern redbelly dace (*Chrosomus eos)*, plains topminnow (*Fundulus sciadicus*), and Iowa darter (*Etheostoma exile*), whose populations have decreased since the early 1990s due to diversion structures and possibly predation by non-native brown trout (Haworth & Bestgen, 2024). Although it is not surprising for fine sediment deposition to occur in the low gradient transition zone, the nature of the deposits seems to reduce or fully block important off-channel habitat units.

Figure 21. Fine sediment deposition in backwaters in the transition zone. A & B) backwaters at site T12 (Archery Range); C) partially filled backwater at site T08; D) filled backwater at site T06. Arrows indicate flow direction of main channel.

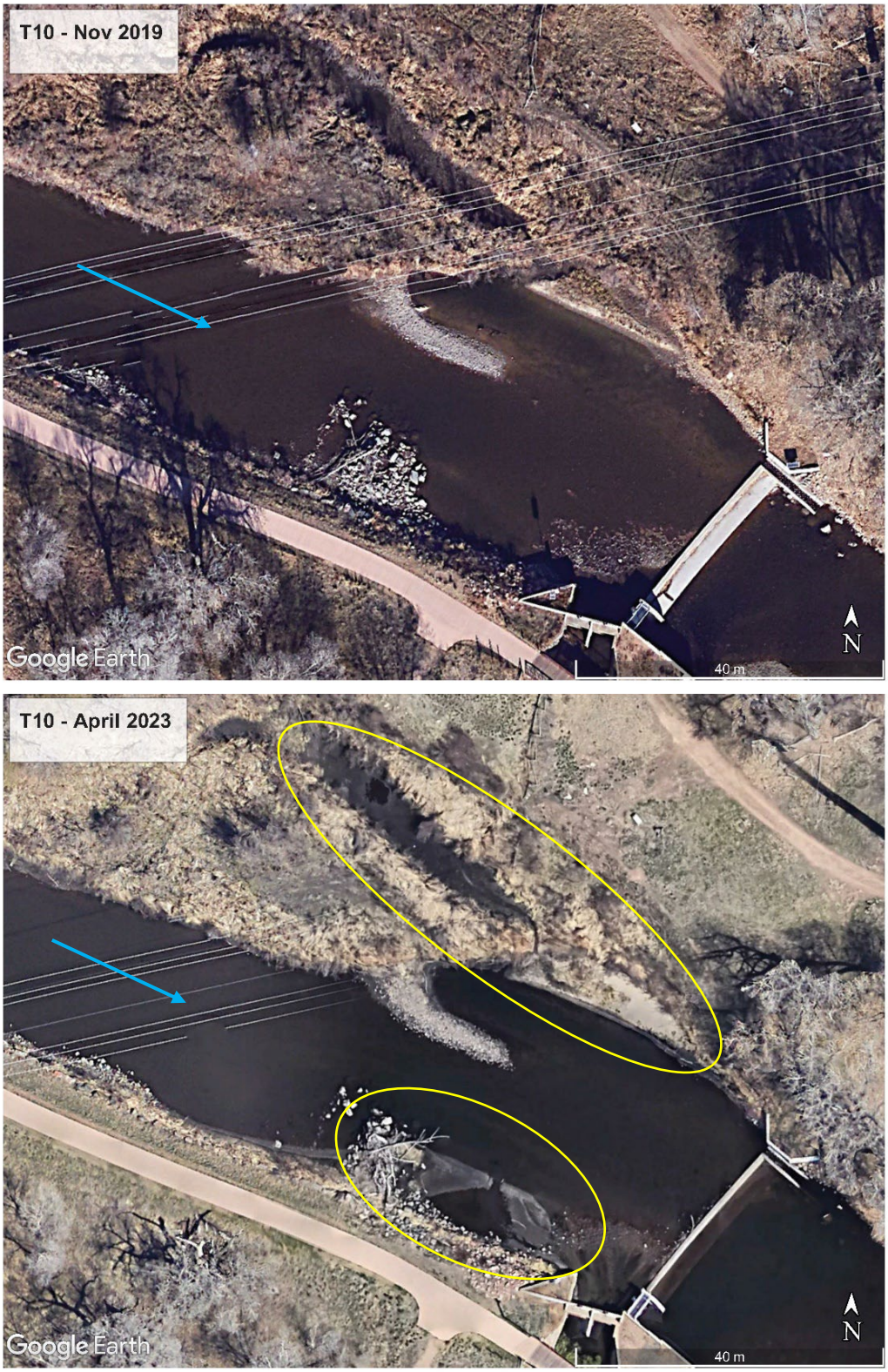

Figure 22. 2019 and 2023 images of site T10 in the transition zone. Blue arrow represents flow direction. Yellow circles show areas of fine sediment deposition and reduction in backwater access on the left bank.

The impact of fine sediment deposition is exacerbated by channel modifications and flow reductions in the transition zone. The river corridor, which includes the channel and floodplain, has been artificially narrowed from both direct channel modifications (bank armor, levees, channel straightening, and diversion dams) and a reduction in flow, which reduces channel width, floodplain area, and geomorphic complexity (Graf, 2006). Bank armoring restricts the river's ability to laterally erode in response to aggradation, a process that leads to higher geomorphic complexity and improves aquatic habitats (Garcia et al., 2012). Channel mobility also improves habitat diversity through localized scour and deposition during meander migration (Choné & Biron, 2016). The presence of logjams promotes bank erosion and overbank flow, which leads to avulsion and multithread channel planforms, further increasing complexity (Collins et al., 2012; Wohl, 2016). The transition zone's reduced geomorphic complexity and lack of lateral mobility restricts the river's ability to respond dynamically to an increased sediment supply resulting from a wildfire (Shanahan et al., 2014). Fine sediment deposition occurs primarily within the main channel and most harmfully in the few off-channel areas (side channels and backwaters) that remain, and their persistence suggests that the channel's artificial stability discourages the erosion and transport of these deposits during normal high flows. Additionally, the persistence of these deposits will encourage vegetation to establish and stabilize them further (Figure 23). I suspect that some large deposits in channel margins, side channels, and backwaters will have long residence times.

Figure 23. Marginal sand deposits with established vegetation. (A) Site T06 (ducks for scale) and (B) Site T12 (Archery Range)

5.2 Embeddedness

Along with reach location and gradient, cross-sectional area correlates positively with embeddedness ($R^2 = 0.23$, $p = 0.05$; Figure 11). This indicates that low-velocity reaches are more likely to retain fines in the substrate. Additionally, multiple linear regression analysis of embeddedness as a function of bedform at the transect level indicates that pools have the highest embeddedness of main channel bedforms. In pool-riffle channels, pools have been shown to fill with fine sediment in response to increased sediment load (Lisle, 1982; Lisle & Hilton, 1992, 1999), but pool-riffle morphology can be resilient to changes in flow and sediment supply (Hassan et al., 2021; Lei et al., 2023). Although I did not measure changes to pool-riffle morphology, I did not notice any pools that lost significant volume due to fine sediment deposition. This leads me to believe that overall pool-riffle morphology has been resilient since the fire, but pools preferentially store fine sediment. This conclusion agrees with Milan & Large (2014), who observed preferential sand storage in pools in a regulated, straightened channel, and on bars and riffle margins in an unregulated, sinuous channel.

The high variation of embeddedness in side channels reflect the variable geomorphic conditions throughout the study area. Generally, side channels in the canyon are rarer, have higher gradient, retain flow during low flows, and are less likely to be depositional than side channels in the transition zone. In the transition zone, side channels tend to inundate at high flows and become depositional when flows decrease. All backwaters seemed to be either the location of the former main channel or the mouth of a side channel. Every backwater had 100% embeddedness, meaning fines had accumulated on top of the coarse substrate. The extent of accumulation in backwaters is not captured in the embeddedness metric but can be evaluated qualitatively. The most extreme case is the large backwater at site T06 that completely filled with fines and now cannot connect to the main channel even at high flows (Figure 7), marking a complete loss of key habitat. At other sites, backwaters either became fully or partially

disconnected from the main channel due to deposition at the mouth, or partially filled with fines (Figure 21).

5.3 Spatial Distribution

The spatial distributions of both sediment retention metrics show interesting trends (Figure 9b & 11b). Reach-averaged fine sediment volumes and embeddedness were both significantly higher in the transition zone compared to the canyon reaches downstream of Black Hollow. In the canyon at sites upstream of Black Hollow, volumes were not significantly higher compared to reaches downstream, but embeddedness was statistically significantly higher (at the 0.9 alpha level) in reaches upstream of Black Hollow compared to those downstream within the canyon (Figure 10 and 12). This is noteworthy, given that Black Hollow was a major sediment source for the mainstem. Differences in sediment retention metrics between reaches up and downstream of Black Hollow should be interpreted with caution due to the small sample size (n = 3 upstream, n = 7 downstream). Also, two of the three sites upstream of Black Hollow are low-gradient reaches in wide alluvial valleys and may not represent the full range of channel types.

Both volumes and embeddedness decrease throughout the canyon until the transition zone (Figure 9b & 11b). This could indicate that the fine sediment input from upstream of Black Hollow was high in relation to the debris flow event, and/or that the transport capacity in the canyon increases in the downstream direction and is sufficiently high to move the sediment through the system into the transition zone. Based on the widespread fine sediment deposition in the transition zone combined with high gradients and unaltered flow regime in the canyon, I suspect the canyon is generally a transport reach for post-fire fine sediment.

5.4 Flushing Flows

These spatial trends reflect several concurrent processes dictating fine sediment transport and deposition on the Poudre River. Hydraulic modelling of bed mobilization at different flows validates the spatial distribution of embeddedness seen on the mainstem Poudre River. Differences in embeddedness are further explained by differences in the magnitude, frequency, and duration of peak flows between the canyon and transition zone. The combination of magnitude and frequency of a discharge determines its geomorphic effectiveness, or its ability to do work by transporting sediment (Wolman & Miller, 1960).

Since the Cameron Peak wildfire, canyon sites have experienced more frequent peak flows at the 2- and 5-year recurrence interval level compared to transition zone sites, and those flows have higher bed mobilization potential. This trend is likely the norm over longer timespans, which exacerbates the lack of bed mobilization in the transition zone. Based on historical discharge records from the canyon mouth gauge (United States Geological Survey, 1994; Colorado DWR), the 2-, 5-, and 10-year flood recurrence interval discharges have decreased in the 142 years of record (Table 8). A more natural flow regime existed before 1944, which is when Halligan Reservoir was built on the North Fork Poudre River and four years before the Big Thompson project started diverting water upstream of the canyon mouth (Milhous, 2019). Since then, the 2-, 5-, and 10-year flows at the canyon mouth are roughly 75% of the pre-1944 flows. Even in the heavily altered period since 1944, the canyon mouth experiences considerably higher discharges than the transition zone. For example, the pre-1944 2-year flow (93 m^3/s) is close to the 5-year flow (105 m^3/s) at the Timnath gauge. In general, the average spring peak monthly flow in the transition zone is 59% less than pre-development levels (Shanahan et al., 2014). Recurrence intervals change over time and are dependent on available gauge data, but they can be adequate for revealing long-term flow regimes. Specific recurrence interval flows do not always represent flows such as bankfull or effective discharge and should not be substituted for those flows (Williams, 1978).

Table 9. Comparison of flood frequencies between Canyon Mouth and Timnath gauges.

		Discharge (cms)		
Gauge	**Time Period**	**2-yr**	**5-yr**	**10-yr**
Canyon Mouth	All	84	135	174
	pre 1944	93	153	199
	post 1944	76	118	149
USGS - Timnath	post 1980	54	105	143

The canyon reaches downstream of Black Hollow, which are represented by Indian Meadows in the hydraulic modelling, showed the highest bed mobilization (31%) at the 2-year recurrence interval flow, which is roughly bankfull. Although there is no hard-and-fast rule for what defines a flushing flow based on the proportion of the channel above the critical shear stress, the extent of the channel showing potential bed mobilization indicates that the 2-year flow at Indian Meadows can be considered a flushing flow for removing interstitial fines as defined by Kondolf & Wilcock (1996) (Figure 17). This agrees with Andrews (1984), who determined that the bankfull flow exceeded the threshold of entrainment for the median particle diameter in a study of 24 gravel-bed rivers with minimal flow regulation in the Rocky Mountains of Colorado. The study also showed that bed mobilization was a relatively frequent event and that bankfull discharges occurred on average 0.44 to 22 days per year, or 8.1 days on average. This aligns with flow that has occurred in the canyon reaches (14 days total between 2021 and 2023; 4.33 days per year). Additionally, Emmett & Wolman (2001) found in similar sized gravel-bed streams of the Intermountain West that the bankfull flow correlates to the effective discharge, which is the flow that transports the most sediment. The high frequency and mobilization potential of the bankfull flow is only the case at Indian Meadows and agrees with the speculation that steep canyon reaches are supply limited, transport reaches.

On the other hand, the lack of bed mobilization at the 2-year flow in the transition zone highlights the disequilibrium of the flow regime. The 2-year flow at transition zone sites, which also aligned with bankfull, resulted in 3% or less of the channel experiencing bed mobilization. At those sites, fines on the

surface may be flushed during peak flows, but not from the interstices of the coarse substrate. With continued high sediment supply, fines may be deposited again during the waning limb of the spring peak. Between the two transition zone sites, bed mobilization at Shields Street increases significantly at the 5- and 10-year flows, whereas the Archery Range only has incremental increases (Figure 15). The 5-year flow at Shields Street could be considered a flushing flow because the model shows bed mobilization in the riffles. At the Archery Range, the modelled 10-year flow shows bed mobilization at 20% of the channel area, but it is difficult to say whether this constitutes a reach-wide flushing flow. I credit the discrepancy between the two transition zone sites to the higher slope and lateral confinement at Shields Street that facilitates greater shear stresses and sediment transport potential. Overall, the infrequent occurrence and reduced mobilization potential of flows in the transition zone will exacerbate differences in embeddedness between the canyon and transition zone.

Shanahan et al. (2014) developed an ecological response model (ERM) of the Poudre River in the transition zone that tested the effects of past, present, and potential flow regimes on ecological and geomorphic conditions. Part of that study included determining flushing flows for three objectives, one being the "initial movement of armor and substrate cleaning". In their study, Reach 3a corresponds to Shields Street and Reach 7 corresponds to the Archery Range. The estimated flushing flow discharges for bed mobilization, which had lower and upper bounds of τ_* of 0.035 and 0.06, respectively, are shown in Table 10. The 5-year flow at Shields Street (112 m^3/s or 3,955 ft^3/s), which shows widespread bed mobilization, falls within the bounds of initial bed mobilization at Reach 3a (93 – 195 m^3/s or 3,300 – 6,900 ft^3/s). At Reach 7, which corresponds to the Archery Range, the bounds of initial bed mobilization are 59 – 260 m^3/s (2,100 – 9,200 ft^3/s). My results indicate the 10-year flow at the Archery Range (143 m^3/s or 5,050 ft^3/s) only mobilizes 20% of the bed, so mobilization likely occurs much less frequently there than at Shields Street.

Table 10. Discharge in m^3/s (ft^3/s) corresponding to three thresholds of dimensionless shear stress at the three study locations in Shanahan et al. (2014). τ of 0.035 and 0.06 are lower and upper bounds of initial movement of armor and substrate cleaning. Bolded values are comparable to Shields Street (Reach 3a) and Archery Range (Reach 7) in this study. Adapted from Shanahan et al., 2014, Table II.7*

Location	τ* = 0.021	τ* = 0.03	τ* = 0.035	τ* = 0.06
Reach 3a: Taft to Shields	50 (1,750)	76 (2,700)	**93 (3,300)**	**195 (6,900)**
Reach 3b: Shields to College	40 (1,400)	71 (2,500)	91 (3,200)	227 (8,000)
Reach 7: Boxelder Gauge to I-25	25 (900)	44 (1,550)	**59 (2,100)**	**261 (9,200)**

Shanahan et al. (2014) also suggests that the altered flow regime of the transition zone has led to armoring of the bed and an increase in substrate size, which would also increase the critical shear stress required for bed mobilization. Although the change in grain size is unknown, it is a plausible factor in explaining the lack of mobilization in the transition zone.

An interesting result from the hydraulic modeling was the absence of bed mobilization at Pasquinels Cabin. The site has low gradient and is in a wide alluvial valley, so it is likely to be depositional, but it is surprising that the modelled 10-year flow does not produce bed mobilization. The site had relatively high embeddedness (56%) but low reach-averaged volume, so I expected low to moderate bed mobilization from the models.

5.5 Wildfire

I have quantified the spatial distribution of fine sediment retention and conducted a hydraulic study of bed mobilization to determine the drivers and mobilization potential of fine sediment retention on the Poudre River, but there are still many unanswered questions regarding the mechanisms of the sediment transport like the quantity of continued fine sediment export from the burned area, the degree of fine sediment transport and storage throughout the study area, and amount of bedload transportation at the modelled flows, for example. It is apparent that the Black Hollow debris flow caused major transport and deposition of fine sediment, as seen in Figures 21, 22, and 23 (M. Haworth,

personal communication, April 2024), but fine sediment levels were also sufficiently high upstream of Black Hollow to create embeddedness and marginal deposition. Median turbidity values spiked in the years following the fire and are still above baseline levels, indicating that fine sediment levels are probably still high (Heath & Thorp, 2023). Because my study does not have data through time, it is difficult to discern the fluctuations in fine sediment transport since the fire and the relative effect of the Black Hollow debris flow compared to elevated levels of background fine sediment from the burned area.

Regardless of the source of fine sediment, my findings and noted hydrologic changes (BAER, 2020; Fairchild, 2021; McGrath et al., 2023; Miller, 2022) indicate that fines are easily delivered to the mainstem Poudre River and transported downstream. I posit that the proximity of the Cameron Peak wildfire to the mainstem and its canyon tributaries created the opportunity for direct delivery of fine sediment from lower-order headwaters streams directly into the mainstem, which is a fourth-order stream at the uppermost reach of the study area. There seem to be few opportunities for flow attenuation and sediment storage in these headwaters streams before entering the mainstem and therefore increased longitudinal connectivity of fluxes. Once in the mainstem Poudre River, the high transport capacity enables the efficient transport of fine sediment through the canyon to the transition zone where reduced streamflow leads to deposition.

The response of the Poudre River to increased water and sediment fluxes following the Cameron Peak wildfire emphasizes that resilient stream segments in lower-order tributaries that retain sediment, such as beaver meadows and beads (low gradient, alluvial reaches with accessible floodplains), are necessary to reduce impacts from wildfire on downstream waterways.

5.6 The Future of the Poudre River

Channelization and flow reductions in the transition zone have drastically altered the geomorphological form and function of the Poudre River, and thus, the aquatic ecosystems that evolved with it. Neither of these impacts will go away in the future, but they have very different outlooks. Reestablishing natural river dynamics by reconnecting floodplains and allowing lateral mobility in the historical river corridor through river restoration has the potential to improve ecological conditions, but water use is a different story. Water use is projected to increase on the Poudre River as Front Range communities continue to grow. The Northern Integrated Supply Project (NISP), which is in progress, is a major water supply project that includes two new off-channel reservoirs, one of which (Glade Reservoir) is 170,000 acre-feet (approximately 210 million cubic meters). NISP has obtained water rights to fill Glade Reservoir with Poudre River water during peak spring and summer flows. The Final Environmental Impact Statement (FEIS) states that diversion to fill these reservoirs during peak flows will not affect flushing flows or channel structure, but these claims are heavily disputed (City of Fort Collins, 2018). The City of Fort Collins' comments to the NISP FEIS claims that FEIS uses either the 2-year flow or 1D shear stress calculations for gravel sized particles (2-64 mm), which is not always the median grain size for each site, for their flushing flow criteria. This study has shown that the 2-year flow in the transition zone is not capable of mobilizing the channel substrate to free the embedded interstitial fines, and that the 5-year flow is an adequate flushing flow in the upstream portion of the transition zone, but not downstream. Assuming each of these flood recurrence intervals will decrease in magnitude with increasing water diversions, flushing flows will become rarer and aquatic ecosystems will face increasing stress.

The City of Fort Collins' comments to the FEIS also indicate that NISP will exacerbate a biofeedback loop occurring on the Poudre River in the transition zone that consists of channel narrowing due to reduced flows, vegetation encroachment, and increased flood potential due to greater channel

roughness. Bestgen et al. (2020) and Shanahan et al. (2014) developed an Ecological Response Model (ERM) for the Poudre River's transition zone that evaluates "future trajectories and complex and interacting biophysical functions under various Poudre River flow regimes." The ERM uses cause-and-effect relationships between flow regime, sediment, temperature, and ecological states to predict responses to nine hydrologic scenarios that include three historical scenarios, two future scenarios with reduced availability, and four designed flow regimes to achieve specific ecosystem goals. Unsurprisingly, historical flow regimes resulted in more favorable conditions than present operations and were also much better than future operations with additional water development and a dry climate scenario. Of the designed flow regimes, ones with low and moderate peak flows led to worse outcomes than those with high peak flow, even with dry base flows (Figure 24). Specifically, channel structure scores were highest under reconstructed native and designed scenarios with high peak flows lasting for a minimum of three days that provide flushing flows through coarse substrate mobilization. Interestingly, the moderate peak and high base flow designed scenario (total annual volume of 16.3 thousand ha-m) resulted in worse outcomes than the high peak dry base flow designed scenario (total volume of 11.9 thousand ha-m). Given that the present-day operations have a total annual volume of 8.9 thousand ha-m, the ERM shows that flow scenarios with only slight increases in annual water volume that maintain high peak flows can facilitate frequent bed mobilization and result in positive geomorphic and ecologic outcomes.

The future flow scenario of "additional water development" (Figure 24) is primarily based on the proposed water withdrawals due to NISP, which will reduce peak flows from their current levels (Bestgen et al., 2020; Appendix S2). The primary mitigation of NISP includes increasing base flows which can increase ecosystem function and reduce desiccation in dry years, but this study and results from the ERM indicate the necessity of high peak flows. Another part of NISP's mitigation plan includes peak flow bypasses, but these will only occur when Glade Reservoir is greater than 75% full, which is only

predicted to occur in 43% of the years (Bestgen et al., 2020; Appendix S2). During the years where this is not met, the largest peak flow proposed to pass the diversion is 80 m^3/s and lasts for a maximum of 2 days, which does not meet the thresholds to maintain critical river ecosystem functions. In the transition zone, 80 m^3/s is between the 2- and 5-year flow and may initiate some mobilization at Shields Street, but not at Archery Range (Figure 16; Table 7). On top of that, these flow scenarios are only developed for the diversion point to fill Glade Reservoir which is near the canyon mouth, and they do not account for the major diversions downstream in the transition zone, so downstream reaches (e.g., Archery Range) will have even lower peak flows. Bestgen et al. (2020; Appendix S2) recommend investigating the feasibility of providing coordinated bypasses to meet recommended peak flow magnitudes and durations to support ecosystem function in the Poudre River. Achieving the desired flow magnitudes and durations would require coordination from all diversion operators along the river along with coordinated releases from reservoirs.

Implementing designed flows have been shown to improve downstream conditions for fish and aquatic ecosystems (Gido & Propst, 2012; Kiernan et al., 2012; Marchetti & Moyle, 2001; Propst & Gido, 2004), but this is usually achieved by releases from a single large dam. In the case of the Poudre River, the numerous water users and points of diversion pose a difficult path towards providing holistic river flows that benefit aquatic ecosystems while balancing human water needs.

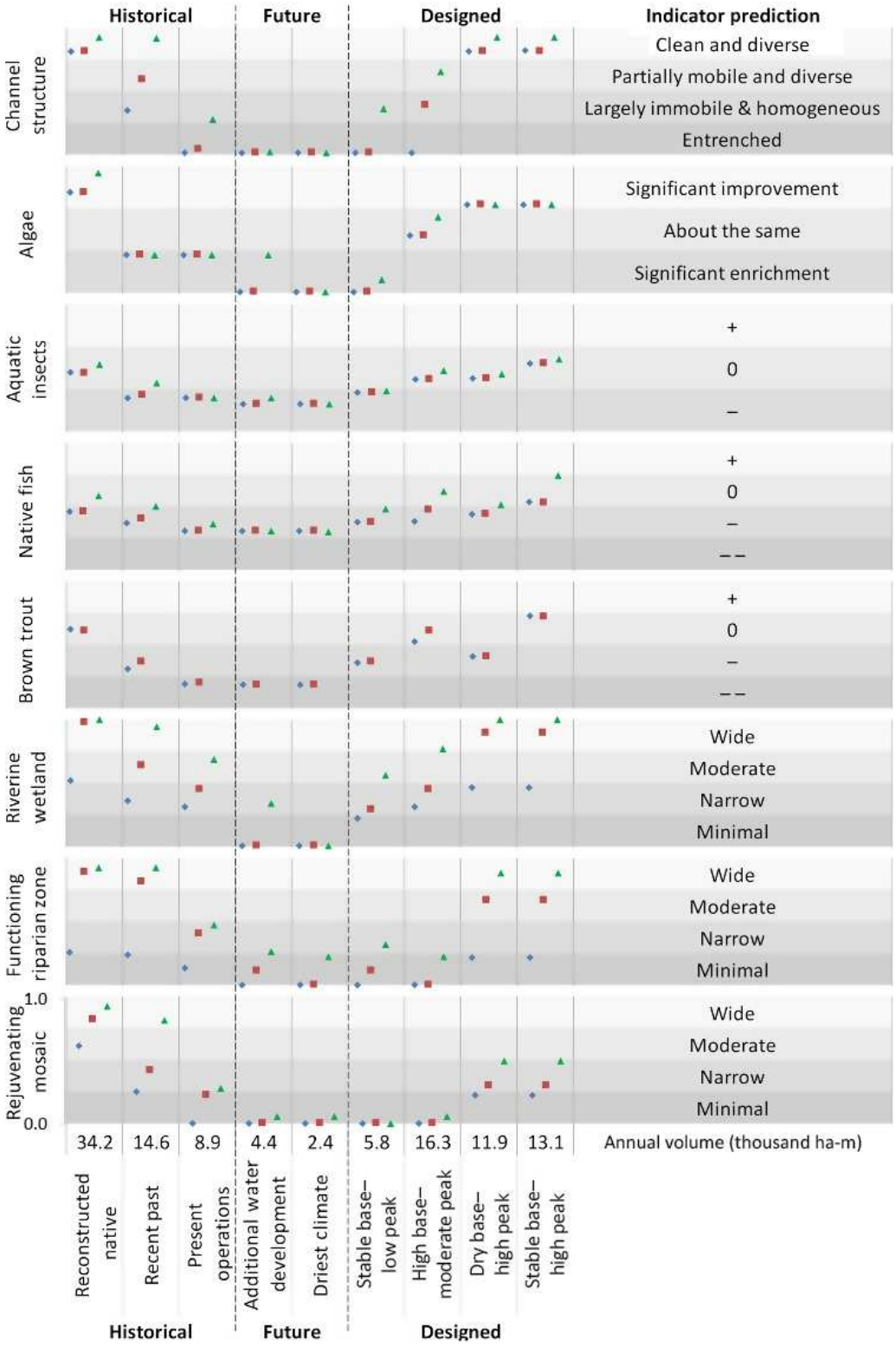

Figure 24. Results of Ecological Response Model (ERM) from Bestgen et al., 2020 (Figure 6), showing responses of eight indicators to three historical, two future, and four designed hydrologic scenarios at three Poudre River reaches. Each indicator is scaled from 0 to 1, with the four different gray-shaded rows for each indicator showing quartiles of change. From up to downstream, blue diamonds are for the confined reach, red squares for the moderately confined reach, and green triangles for the least confined reach.

6. CONCLUSION

The Cameron Peak wildfire of 2020 led to widespread but varied detrimental effects throughout the Poudre River watershed. Excess fine sediment eroded from burned tributaries, combined with the acute devastation from the Black Hollow debris flow, caused loss of life and harmed aquatic ecosystem function and water resources on the mainstem Poudre. The magnitude and distribution of post-fire fine sediment deposition in the mainstem Poudre River reflect the immense size and scale of the fire, varying watershed properties, and human alterations to river. Although the fire occurred in high elevations, the greatest effects were seen in the downstream portion of the study area, which is characterized by altered river form and decreased flow.

Fine sediment retention, when measured by reach-averaged fine sediment volume and embeddedness, is greatest in the transition zone. Both geomorphic position (canyon versus transition zone) and reach-scale geometries are significant predictors of fine sediment retention, but model ranking based on AIC_c reveals geomorphic position is the stronger predictor. Models with cross-sectional area as a predictor of embeddedness are considered substantial, and models with bank length ratio as a predictor of deposit volumes are also supported, albeit to a lesser degree. Embeddedness levels at the transect level indicate that, in main channel bedforms, fine sediment is preferentially retained in pools.

Overall, the greater influence of reach location on both metrics of fine sediment retention indicates watershed-scale processes like geomorphic setting and flow regime are the primary driver for the spatial distribution of fine sediment retention on the Poudre River following the Cameron Peak Wildfire. Hydraulic modelling of flushing flow requirements at four sites spanning the diverse geomorphic settings and flow regimes may point to the mechanisms for differential fine sediment retention, and they can illuminate the potential outcomes as the river recovers from the fire. Modelling results indicate that high gradient reaches in the canyon have a readily mobile bed, while transition zone reaches mobilize less frequently. This likely explains the differences in embeddedness seen between the canyon and

transition zone reaches, and it suggests that in the future, canyon reaches will be able to flush the fines from the channel substrate while the transition zone may retain them longer. With decreased peak flows, reduced lateral mobility, and less floodplain access, detrimental ecological effects from excess fine sediment may be prolonged in the transition zone. This study corroborates the idea that impaired Poudre River function diminishes geomorphic and ecological resilience to disturbances such as wildfires.

6.1 Future Work

This thesis is part of a larger project that also includes monitoring fish population recovery from the 2021 fish kill in the canyon and transition zone, monitoring the passage rates of fish at diversions with fish passage structures, and monitoring success of rare fish recovery efforts. Results from this thesis may help explain rates of fish recovery and ecologic integrity throughout the study area.

There are many ways to expand upon the findings of this thesis. First, data were collected during one season, three years after the fire, so temporal trends can only be inferred based on spatial distribution of fine sediment retention. Repeat surveys would be able to discern whether the sediment is being flushed or accumulating in different portions of the study area. Due to the systematic nature of the transect surveys, it would be easy to repeat the embeddedness and substrate size surveys to compare between years. I assume the bankfull cross-sectional topography is generally stable, so that portion of the survey would not need to be repeated every year.

The most useful way to monitor the metric of fine sediment volume would be to identify large deposits occupying critical habitat features (backwaters, side channels, margins) and conduct repeat volume and RTK or drone surveys. This could be expanded to all 13 CSU Larval Fish Laboratory fish monitoring sites in the transition zone or anywhere that fine sediment is occupying key habitats. The results of this thesis make it clear that the transition zone is the primary site for large sand deposits, so I

would recommend focusing detailed monitoring efforts there with some reconnaissance level monitoring in the canyon if another sediment deposition event occurs.

Hydraulic modelling of flushing flows could also be expanded. Water-surface elevations at multiple discharges and precise sediment size distributions would increase the accuracy of the models used to estimate bed mobilization. The methods used in this study do not yield substrate size data useful for estimating sediment size distribution, which can provide a more accurate indicator of bed sorting. Mapping substrate size at the channel unit or bedform level may be a better approach than using a reach averaged D_{50}. Also, there are methods for determining substrate size from drone-based orthophotos, which could yield results with higher spatial resolution.

At sites with large fine sediment volumes, such as the Archery Range, hydraulic modelling could be used to determine the flows required to remobilize individual deposits. I focused on bed mobilization because it could reveal differences in embeddedness and was testable at all sites.

Quantifying the magnitude, frequency, and duration of flushing flows is important for understanding outcomes for the aquatic ecosystem of the Poudre River, especially given that there are plans for a new off-channel reservoir that will be filled by withdrawing water from the Poudre River during peak flows.

6.2 Potential Mitigation Measures

As discussed in Section 5.6, the future of the Poudre River's ecologic and geomorphic integrity depends on the river's ability provide ecological functions associated with its natural flow regime. With the high likelihood of continued reduced peak flows in the transition zone, there are other mitigation measures that can be taken on the reach scale to reduce impacts to aquatic ecosystems from future events like wildfires and debris flows. These include changes to channel form that allow beneficial functions to occur even with reduced flow. In laterally restricted reaches, removing constrictions such as levees and armored banks would allow the river to erode its banks and develop an appropriate width

based on the current flow regime. Additionally, designing reaches to have multiple floodplain surfaces (benches) would initiate floodplain processes at lower flows and promote fine sediment deposition away from the main channel bottom in the case of another large sediment pulse. Increasing geomorphic heterogeneity may initiate localized scour and deposition, rather than reach-wide deposition, and combined with less restrictive banks, would increase a reach's resilience to a sediment pulse by being able to adjust its channel boundaries. Increased geomorphic heterogeneity can be achieved by designing reaches to have islands, side channels, bars, and log jams.

The measures I describe are only possible in reaches where the river corridor (the active channel and floodplains) can be extended laterally. This is rare in a partially urbanized, populated river corridor, but it is possible. For example, a recent river restoration project at site T11 to improve the City of Fort Collins' water intake also included the installation of large wood structures on a point bar to promote localized deposition and heterogeneity, as well as re-grading parts of the channel and banks to promote floodplain inundation, bank erosion, and the creation of channel margin habitats like backwaters. Since its completion in 2023, microhabitats associated with the wood structures have been observed, and small-bodied native fish were found using the created channel margin habitat (Haworth, personal communication, June 2024). Overall patch density (i.e., heterogeneity) has increased, and aggradation is occurring in patches throughout the reach rather than large accumulations that reduce habitats like backwaters and side channels (Schoner, personal communication, June 2024).

Ideally, this reach will be able to deposit and retain sediment in a beneficial way that creates habitat heterogeneity rather than filling in and reducing key habitats. However, a single resilient reach among many poorly functioning ones will not resolve the issues of the transition zone, so it is important to promote similar restoration projects in a longitudinal series, like beads on a string, to create a watershed-scale effect.

In final, the severely impacted backwaters (Figure 7, 21, & 22) in the transition zone may need mechanical removal of accumulated fine sediment to restore the lost habitat. After two years of spring snowmelt, the deposits appear to be quite stable and may only remobilize during extreme floods. Over time, these deposits could become vegetated, stabilized, and accreted to the bank. Although using heavy equipment in or near the river can be harmful, it seems to be a necessary response to such a drastic event.

REFERENCES

Ader, E., Wohl, E., McFadden, S., & Singha, K. (2021). Logjams as a driver of transient storage in a mountain stream. *Earth Surface Processes and Landforms*, *46*(3), 701–711. https://doi.org/10.1002/esp.5057

Andrews, E. D. (1984). Bed-material entrainment and hydraulic geometry of gravel-bed rivers in Colorado. *Geological Society of America Bulletin*, *95*(3), 371. https://doi.org/10.1130/0016-7606(1984)95<371:BEAHGO>2.0.CO;2

BAER. (2020). *BAER - Cameron Peak Fire Forest Service Burned Area Emergency Response Executive Summary*. Arapaho Roosevelt National Forest.

Barton, K. (2023). *MuMIn: Multi-Model Inference* (R package version 1.47.5) [Computer software]. https://CRAN.R-project.org/package=MuMIn

Battige, K. (2022). *Cache la Poudre River Fish Survey and Management Information*. Colorado Parks and Wildlife. https://cpw.state.co.us/thingstodo/Fishery%20Survey%20Summaries/CachelaPoudreRiverCanyon.pdf

Benavides-Solorio, J., & MacDonald, L. H. (2001). Post-fire runoff and erosion from simulated rainfall on small plots, Colorado Front Range. *Hydrological Processes*, *15*(15), 2931–2952. https://doi.org/10.1002/hyp.383

Benda, L., Miller, D., Bigelow, P., & Andras, K. (2003). Effects of post-wildfire erosion on channel environments, Boise River, Idaho. *Forest Ecology and Management*, *178*(1–2), 105–119. https://doi.org/10.1016/S0378-1127(03)00056-2

Bestgen, K. R., Poff, N. L., Baker, D. W., Bledsoe, B. P., Merritt, D. M., Lorie, M., Auble, G. T., Sanderson, J. S., & Kondratieff, B. C. (2020). Designing flows to enhance ecosystem functioning in heavily altered rivers. *Ecological Applications*, *30*(1). https://doi.org/10.1002/eap.2005

Bixby, R. J., Cooper, S. D., Gresswell, R. E., Brown, L. E., Dahm, C. N., & Dwire, K. A. (2015). Fire effects on aquatic ecosystems: An assessment of the current state of the science. *Freshwater Science*, *34*(4), 1340–1350. https://doi.org/10.1086/684073

Brogan, D. J., Nelson, P. A., & MacDonald, L. H. (2019). Spatial and temporal patterns of sediment storage and erosion following a wildfire and extreme flood. *Earth Surface Dynamics*, *7*(2), 563–590. https://doi.org/10.5194/esurf-7-563-2019

Burnham, K. P., & Anderson, D. R. (2002). *Model selection and multimodel inference: A practical information-theoretic approach* (2nd ed). Springer.

Carrivick, J. L., & Smith, M. W. (2019). Fluvial and aquatic applications of Structure from Motion photogrammetry and unmanned aerial vehicle/drone technology. *WIREs Water*, *6*(1), e1328. https://doi.org/10.1002/wat2.1328

Choné, G., & Biron, P. M. (2016). Assessing the Relationship Between River Mobility and Habitat. *River Research and Applications*, *32*(4), 528–539. https://doi.org/10.1002/rra.2896

Church, M., Wolcott, J. F., & Fletcher, W. K. (1991). A Test of Equal Mobility in Fluvial Sediment Transport: Behavior of the Sand Fraction. *Water Resources Research*, *27*(11), 2941–2951. https://doi.org/10.1029/91WR01622

City of Fort Collins. (2017). *State of the Poudre River*. https://www.fcgov.com/poudrereportcard/

City of Fort Collins. (2018). *Comments on the Final Environmental Impact Statement for the Northern Integrated Supply Project*. https://www.fcgov.com/nispreview/files/nisp-feis-comments-2018-10-4.pdf?1618443216

Collins, B. D., Montgomery, D. R., Fetherston, K. L., & Abbe, T. B. (2012). The floodplain large-wood cycle hypothesis: A mechanism for the physical and biotic structuring of temperate forested alluvial valleys in the North Pacific coastal ecoregion. *Geomorphology*, *139–140*, 460–470. https://doi.org/10.1016/j.geomorph.2011.11.011

Cover, M. R., May, C. L., Dietrich, W. E., & Resh, V. H. (2008). Quantitative linkages among sediment supply, streambed fine sediment, and benthic macroinvertebrates in northern California streams. *Journal of the North American Benthological Society*, *27*(1), 135–149. https://doi.org/10.1899/07-032.1

David, C. G., Kohl, N., Casella, E., Rovere, A., Ballesteros, P., & Schlurmann, T. (2021). Structure-from-Motion on shallow reefs and beaches: Potential and limitations of consumer-grade drones to reconstruct topography and bathymetry. *Coral Reefs*, *40*(3), 835–851. https://doi.org/10.1007/s00338-021-02088-9

De Cicco, L. A., Hirsch, R. M., Lorenz, D., Watkins, D., & Johnson, M. (2018). *DataRetrieval* [Computer software]. [object Object]. https://doi.org/10.5066/P9X4L3GE

Dennison, P. E., Brewer, S. C., Arnold, J. D., & Moritz, M. A. (2014). Large wildfire trends in the western United States, 1984–2011. *Geophysical Research Letters*, *41*(8), 2928–2933. https://doi.org/10.1002/2014GL059576

Dey, S., & Ali, S. Z. (2019). Bed sediment entrainment by streamflow: State of the science. *Sedimentology*, *66*(5), 1449–1485. https://doi.org/10.1111/sed.12566

Díaz-Raviña, M., Martín, A., Barreiro, A., Lombao, A., Iglesias, L., Díaz-Fierros, F., & Carballas, T. (2012). Mulching and seeding treatments for post-fire soil stabilisation in NW Spain: Short-term effects and effectiveness. *Geoderma*, *191*, 31–39. https://doi.org/10.1016/j.geoderma.2012.01.003

Dietrich, J. T. (2017). Bathymetric Structure-from-Motion: Extracting shallow stream bathymetry from multi-view stereo photogrammetry. *Earth Surface Processes and Landforms*, *42*(2), 355–364. https://doi.org/10.1002/esp.4060

Dunn, S. B. (2023). *Dammed Ponds! A study of postfire sediment* [Master's Thesis]. Colorado State University.

Emelko, M. B., Stone, M., Silins, U., Allin, D., Collins, A. L., Williams, C. H. S., Martens, A. M., & Bladon, K. D. (2016). Sediment-phosphorus dynamics can shift aquatic ecology and cause downstream legacy effects after wildfire in large river systems. *Global Change Biology*, *22*(3), 1168–1184. https://doi.org/10.1111/gcb.13073

Emmett, W. W., & Wolman, M. G. (2001). Effective discharge and gravel-bed rivers. *Earth Surface Processes and Landforms*, *26*(13), 1369–1380. https://doi.org/10.1002/esp.303

Escobar-Arias, M. I., & Pasternack, G. B. (2010). A hydrogeomorphic dynamics approach to assess in-stream ecological functionality using the functional flows model, part 1-model characteristics. *River Research and Applications*, *26*(9), 1103–1128. https://doi.org/10.1002/rra.1316

Fairchild, M. (2021). *FINAL FISHERIES SPECIALIST REPORT (ROUND 2, FINAL) CAMERON PEAK FIRE: BURNED AREA EMERGENCY RESPONSE (BAER) ASSESSMENT ARAPAHO & ROOSEVELT NATIONAL FORESTS*. Arapaho & Roosevelt National Forests and Pawnee National Grassland.

Fairfax, E., Whipple, A., Wheaton, J. M., Osorio, B., Miller, J., Kirksey, K., Perez, N., Gilbert, J. T., & Jordan, C. E. (2024). Impacts of beaver dams on riverscape burn severity during megafires in the Rocky Mountain region, western United States. In J. L. Florsheim, A. P. O'Dowd, & A. Chin (Eds.), *Biogeomorphic Responses to Wildfire in Fluvial Ecosystems*. Geological Society of America. https://doi.org/10.1130/2024.2562(07)

Fausch, K. D., & Bestgen, K. R. (1997). Ecology of Fishes Indigenous to the Central and Southwestern Great Plains. In F. L. Knopf & F. B. Samson (Eds.), *Ecology and Conservation of Great Plains Vertebrates* (Vol. 125, pp. 131–166). Springer New York. https://doi.org/10.1007/978-1-4757-2703-6_6

Florsheim, J. L., & Chin, A. (2022). Geomorphic Responses to Wildfire in Fluvial Systems. In *Treatise on Geomorphology* (pp. 478–503). Elsevier. https://doi.org/10.1016/B978-0-12-818234-5.00045-6

Garcia, X.-F., Schnauder, I., & Pusch, M. T. (2012). Complex hydromorphology of meanders can support benthic invertebrate diversity in rivers. *Hydrobiologia*, *685*(1), 49–68. https://doi.org/10.1007/s10750-011-0905-z

Gido, K. B., & Propst, D. L. (2012). Long-Term Dynamics of Native and Nonnative Fishes in the San Juan River, New Mexico and Utah, under a Partially Managed Flow Regime. *Transactions of the American Fisheries Society*, *141*(3), 645–659. https://doi.org/10.1080/00028487.2012.683471

Gomez Isaza, D. F., Cramp, R. L., & Franklin, C. E. (2022). Fire and rain: A systematic review of the impacts of wildfire and associated runoff on aquatic fauna. *Global Change Biology*, *28*(8), 2578–2595. https://doi.org/10.1111/gcb.16088

Graf, W. L. (2006). Downstream hydrologic and geomorphic effects of large dams on American rivers. *Geomorphology*, *79*(3–4), 336–360. https://doi.org/10.1016/j.geomorph.2006.06.022

Gresswell, R. E. (1999). *Fire and Aquatic Ecosystems in Forested Biomes of North America*.

Hassan, M. A., Radić, V., Buckrell, E., Chartrand, S. M., & McDowell, C. (2021). Pool-Riffle Adjustment Due to Changes in Flow and Sediment Supply. *Water Resources Research*, *57*(2). https://doi.org/10.1029/2020WR028048

Haworth, M. R., & Bestgen, K. R. (2024). Low-head dam fragmentation, habitat alteration, and invasive predators degrade a Western United States stream fish assemblage. *Ecology of Freshwater Fish*, e12773. https://doi.org/10.1111/eff.12773

Heath, J., & Thorp, R. (2023). *WATER QUALITY TRENDS REPORT 2008 – 2022 Upper Cache la Poudre Watershed Collaborative Water Quality Monitoring Program*. City of Fort Collins Utilities - Water Quality Services Division.

Jarrett, R. D. (1990). Paleohydrologic techniques used to define the spatial occurrence of floods. *Geomorphology*, *3*(2), 181–195. https://doi.org/10.1016/0169-555X(90)90044-Q

Julien, P. Y. (2010). *Erosion and Sedimentation* (2nd ed.). Cambridge University Press. https://doi.org/10.1017/CBO9780511806049

Kemp, P., Sear, D., Collins, A., Naden, P., & Jones, I. (2011). The impacts of fine sediment on riverine fish. *Hydrological Processes*, *25*(11), 1800–1821. https://doi.org/10.1002/hyp.7940

Kiernan, J. D., Moyle, P. B., & Crain, P. K. (2012). Restoring native fish assemblages to a regulated California stream using the natural flow regime concept. *Ecological Applications*, *22*(5), 1472–1482. https://doi.org/10.1890/11-0480.1

Komar, P. D. (1987). Selective gravel entrainment and the empirical evaluation of flow competence. *Sedimentology*, *34*(6), 1165–1176. https://doi.org/10.1111/j.1365-3091.1987.tb00599.x

Kondolf, G. M., & Wilcock, P. R. (1996). The Flushing Flow Problem: Defining and Evaluating Objectives. *Water Resources Research*, *32*(8), 2589–2599. https://doi.org/10.1029/96WR00898

Kostelnik, J., Schmitt, R. G., Rengers, F. K., & Kean, J. W. (2021). *Cameron Peak Fire: Flooding and Debris Flows*. https://landslides.usgs.gov/storymap/cameronpeak/

Kunze, M. D., & Stednick, J. D. (2006). Streamflow and suspended sediment yield following the 2000 Bobcat fire, Colorado. *Hydrological Processes*, *20*(8), 1661–1681. https://doi.org/10.1002/hyp.5954

Kuznetsova, A., Brockhoff, P. B., & Christensen, R. H. B. (2017). **lmerTest** Package: Tests in Linear Mixed Effects Models. *Journal of Statistical Software*, *82*(13). https://doi.org/10.18637/jss.v082.i13

Lane, P. N. J., Sheridan, G. J., & Noske, P. J. (2006). Changes in sediment loads and discharge from small mountain catchments following wildfire in south eastern Australia. *Journal of Hydrology*, *331*(3–4), 495–510. https://doi.org/10.1016/j.jhydrol.2006.05.035

Legleiter, C. J., Lawrence, R. L., Fonstad, M. A., Andrew Marcus, W., & Aspinall, R. (2003). Fluvial response a decade after wildfire in the northern Yellowstone ecosystem: A spatially explicit analysis. *Geomorphology*, *54*(3–4), 119–136. https://doi.org/10.1016/S0169-555X(02)00332-X

Lei, Y., Hassan, M. A., Viparelli, E., Chartrand, S. M., An, C., Fu, X., & Hu, C. (2023). The Effect of Sediment Supply on Pool-Riffle Morphology. *Water Resources Research*, *59*(11), e2023WR035983. https://doi.org/10.1029/2023WR035983

Lisle, T. E. (1982). Effects of aggradation and degradation on riffle-pool morphology in natural gravel channels, northwestern California. *Water Resources Research*, *18*(6), 1643–1651. https://doi.org/10.1029/WR018i006p01643

Lisle, T. E., & Hilton, S. (1992). THE VOLUME OF FINE SEDIMENT IN POOLS: AN INDEX OF SEDIMENT SUPPLY IN GRAVEL-BED STREAMS. *Journal of the American Water Resources Association*, *28*(2), 371–383. https://doi.org/10.1111/j.1752-1688.1992.tb04003.x

Lisle, T. E., & Hilton, S. (1999). Fine bed material in pools of natural gravel bed channels. *Water Resources Research*, *35*(4), 1291–1304. https://doi.org/10.1029/1998WR900088

Loáiciga, H. A., Pedreros, D., & Roberts, D. (2001). Wildfire-streamflow interactions in a chaparral watershed. *Advances in Environmental Research*, *5*(3), 295–305. https://doi.org/10.1016/S1093-0191(00)00064-2

Loveland Power and Water. (2023). *Big Thompson River Source Water Quality 2022 Annual Report*. Loveland Power and Water.

Marchetti, M. P., & Moyle, P. B. (2001). EFFECTS OF FLOW REGIME ON FISH ASSEMBLAGES IN A REGULATED CALIFORNIA STREAM. *Ecological Applications*, *11*(2), 530–539. https://doi.org/10.1890/1051-0761(2001)011[0530:EOFROF]2.0.CO;2

McGrath, D., Zeller, L., Bonnell, R., Reis, W., Kampf, S., Williams, K., Okal, M., Olsen-Mikitowicz, A., Bump, E., Sears, M., & Rittger, K. (2023). Declines in Peak Snow Water Equivalent and Elevated Snowmelt Rates Following the 2020 Cameron Peak Wildfire in Northern Colorado. *Geophysical Research Letters*, *50*(6), e2022GL101294. https://doi.org/10.1029/2022GL101294

Milan, D. J., & Large, A. R. G. (2014). Magnetic tracing of fine-sediment over pool-riffle morphology. *CATENA*, *115*, 134–149. https://doi.org/10.1016/j.catena.2013.11.003

Milhous, R. T. (2019). *DETERMINING ENVIRONMENTAL FLOWS FOR FLUSING OF FINES FROM A RIVER: CACHE LA POUDRE, COLORADO USA*. 4802–4811. https://doi.org/10.3850/38WC092019-0673

Miller, Q. (2022). *Streamflow generation across an elevation gradient after the 2020 Cameron peak fire* [Master's Thesis]. Colorado State University.

Minshall, G. W. (2003). Responses of stream benthic macroinvertebrates to fire. *Forest Ecology and Management*, *178*(1–2), 155–161. https://doi.org/10.1016/S0378-1127(03)00059-8

Minshall, G. W., Brock, J. T., & Varley, J. D. (1989). Wildfires and Yellowstone's Stream Ecosystems. *BioScience*, *39*(10), 707–715. https://doi.org/10.2307/1311002

Minshall, G. W., Robinson, C. T., & Lawrence, D. E. (1997). *Postfire responses of lotic ecosystems in Yellowstone National Park, U.S.A. 54*.

Montgomery, D. R., & Buffington, J. M. (1997). Channel-reach morphology in mountain drainage basins. *Geological Society of America Bulletin*, *109*(5), 596–611. https://doi.org/10.1130/0016-7606(1997)109<0596:CRMIMD>2.3.CO;2

Moody, J. A., & Martin, D. A. (2001). Initial hydrologic and geomorphic response following a wildfire in the Colorado Front Range. *Earth Surface Processes and Landforms*, *26*(10), 1049–1070. https://doi.org/10.1002/esp.253

National Oceanic and Atmospheric Administration. (2024, May 30). *Colorado Climate Center*. https://climate.colostate.edu/

Ortega-Becerril, J. A., Suarez, C., Vázquez-Tarrío, D., Garrote, J., & Gomez-Heras, M. (2024). Sediment Response after Wildfires in Mountain Streams and Their Effects on Cultural Heritage: The Case of the 2021 Navalacruz Wildfire (Avila, Spain). *Fire*, *7*(2), 52. https://doi.org/10.3390/fire7020052

Page, K., & Nanson, G. (1982). Concave-bank benches and associated floodplain formation. *Earth Surface Processes and Landforms*, *7*(6), 529–543. https://doi.org/10.1002/esp.3290070603

Parker, G., & Klingeman, P. C. (1982). On why gravel bed streams are paved. *Water Resources Research*, *18*(5), 1409–1423. https://doi.org/10.1029/WR018i005p01409

Parker, G., & Toro-Escobar, C. M. (2002). Equal mobility of gravel in streams: The remains of the day. *Water Resources Research*, *38*(11). https://doi.org/10.1029/2001WR000669

Paul, M. J., LeDuc, S. D., Lassiter, M. G., Moorhead, L. C., Noyes, P. D., & Leibowitz, S. G. (2022). Wildfire Induces Changes in Receiving Waters: A Review With Considerations for Water Quality Management. *Water Resources Research*, *58*(9), e2021WR030699. https://doi.org/10.1029/2021WR030699

Peck, D. V., Lazorchak, J. M., & Klemm, D. J. (2001). *ENVIRONMENTAL MONITORING AND ASSESSMENT PROGRAM - SURFACE WATERS: WESTERN PILOT STUDY FIELD OPERATIONS MANUAL FOR WADEABLE STREAMS* (p. 154). US Environmental Protection Agency.

Poff, N. L., Allan, J. D., Bain, M. B., Karr, J. R., Prestegaard, K. L., Richter, B. D., Sparks, R. E., & Stromberg, J. C. (1997). The Natural Flow Regime. *BioScience*, *47*(11), 769–784. https://doi.org/10.2307/1313099

Polvi, L. E., Nilsson, C., & Hasselquist, E. M. (2014). Potential and actual geomorphic complexity of restored headwater streams in northern Sweden. *Geomorphology*, *210*, 98–118. https://doi.org/10.1016/j.geomorph.2013.12.025

Polvi, L. E., & Wohl, E. (2012). The beaver meadow complex revisited – the role of beavers in post-glacial floodplain development. *Earth Surface Processes and Landforms*, *37*(3), 332–346. https://doi.org/10.1002/esp.2261

Powell, D. M. (1998). Patterns and processes of sediment sorting in gravel-bed rivers. *Progress in Physical Geography: Earth and Environment*, *22*(1), 1–32. https://doi.org/10.1177/030913339802200101

Preston, D. L., Trujillo, J. L., Fairchild, M. P., Morrison, R. R., Fausch, K. D., & Kanno, Y. (2023). Short-term effects of wildfire on high elevation stream-riparian food webs. *Oikos*, *2023*(8), e09828. https://doi.org/10.1111/oik.09828

Propst, D. L., & Gido, K. B. (2004). Responses of Native and Nonnative Fishes to Natural Flow Regime Mimicry in the San Juan River. *Transactions of the American Fisheries Society*, *133*(4), 922–931. https://doi.org/10.1577/T03-057.1

R Core Team. (2021). *R: A language and environment for statistical computing* [Computer software]. R Foundation for Statistical Computing. https://www.R-project.org/

Reale, J. K., Archdeacon, T. P., Van Horn, D. J., Gonzales, E. J., Dudley, R. K., Turner, T. F., & Dahm, C. N. (2021). Differential effects of a catastrophic wildfire on downstream fish assemblages in an aridland river. *Aquatic Ecology*, *55*(2), 483–500. https://doi.org/10.1007/s10452-021-09839-4

Reale, J. K., Van Horn, D. J., Condon, K. E., & Dahm, C. N. (2015). The effects of catastrophic wildfire on water quality along a river continuum. *Freshwater Science*, *34*(4), 1426–1442. https://doi.org/10.1086/684001

Reid, H. E., & Brierley, G. J. (2015). Assessing geomorphic sensitivity in relation to river capacity for adjustment. *Geomorphology*, *251*, 108–121. https://doi.org/10.1016/j.geomorph.2015.09.009

Reneau, S. L., Katzman, D., Kuyumjian, G. A., Lavine, A., & Malmon, D. V. (2007). Sediment delivery after a wildfire. *Geology*, *35*(2), 151. https://doi.org/10.1130/G23288A.1

Ryan, S. E., & Dixon, M. K. (2008). Spatial and temporal variability in stream sediment loads using examples from the Gros Ventre Range, Wyoming, USA. In *Developments in Earth Surface Processes* (Vol. 11, pp. 387–407). Elsevier. https://doi.org/10.1016/S0928-2025(07)11134-2

Ryan, S. E., Dwire, K. A., & Dixon, M. K. (2011). Impacts of wildfire on runoff and sediment loads at Little Granite Creek, western Wyoming. *Geomorphology*, *129*(1–2), 113–130. https://doi.org/10.1016/j.geomorph.2011.01.017

Schmidt, J. C. (1990). Recirculating Flow and Sedimentation in the Colorado River in Grand Canyon, Arizona. *The Journal of Geology*, *98*(5), 709–724. https://doi.org/10.1086/629435

Schumm, S. (1977). *The Fluvial System*. Wiley.

Sexton, J. M. (1998). *The Historical Changes in the Cache La Poudre River, Fort Collins, Colorado* [Master's Thesis]. Colorado State University.

Shanahan, J. O., Baker, D. W., Bledsoe, B. P., Poff, N. L., Merritt, D. M., Bestgen, K. R., Auble, G. T., Kondratieff, B. C., Stokes, J. G., Lorie, M., & Sanderson, J. S. (2014). *An ecological response model for the Cache la Poudre River through Fort Collins* (p. 93). City of Fort Collins Natural Areas Department, Fort Collins, CO. https://www.fcgov.com/naturalareas/eco-response.php

Shelley, J., & Bailey, P. (2018). *The Cross Section Viewer: A Tool for Automating Geomorphic Analysis Using Riverine Cross-Section Data*.

Shields, A. (1936). Application of Similarity Principles and Turbulence Research to Bedload Movement. *Berlin: Wasserbau Schiffbau. (English Translation by Ott, W. P., and van Uchelen, J. C., Hydraulics Laboratory, California Institute of Technology)*, *26*, 5–24.

Smith, H. G., Sheridan, G. J., Lane, P. N. J., Nyman, P., & Haydon, S. (2011). Wildfire effects on water quality in forest catchments: A review with implications for water supply. *Journal of Hydrology*, *396*(1–2), 170–192. https://doi.org/10.1016/j.jhydrol.2010.10.043

Tomkins, K. M., Humphreys, G. S., Gero, A. F., Shakesby, R. A., Doerr, S. H., Wallbrink, P. J., & Blake, W. H. (2008). Postwildfire hydrological response in an El Niño–Southern Oscillation–dominated environment. *Journal of Geophysical Research: Earth Surface*, *113*(F2), 2007JF000853. https://doi.org/10.1029/2007JF000853

United States Geological Survey. (1994). *USGS Water Data for the Nation*. https://doi.org/10.5066/F7P55KJN

US Army Corps of Engineers. (2023). *HEC-RAS User's Manual*. Hydrologic Engineering Center: Davis, CA, USA.

U.S. Geological Survey. (2019). *The StreamStats program* [Computer software]. https://streamstats.usgs.gov/ss/

Walker, B., Holling, C. S., Carpenter, S. R., & Kinzig, A. P. (2004). Resilience, Adaptability and Transformability in Social-ecological Systems. *Ecology and Society*, *9*(2), art5. https://doi.org/10.5751/ES-00650-090205

Westoby, M. J., Brasington, J., Glasser, N. F., Hambrey, M. J., & Reynolds, J. M. (2012). 'Structure-from-Motion' photogrammetry: A low-cost, effective tool for geoscience applications. *Geomorphology*, *179*, 300–314. https://doi.org/10.1016/j.geomorph.2012.08.021

Wilcock, P. R. (1993). Critical Shear Stress of Natural Sediments. *Journal of Hydraulic Engineering*, *119*(4), 491–505. https://doi.org/10.1061/(ASCE)0733-9429(1993)119:4(491)

Wilcock, P. R., & Crowe, J. C. (2003). Surface-based Transport Model for Mixed-Size Sediment. *Journal of Hydraulic Engineering*, *129*(2), 120–128. https://doi.org/10.1061/(ASCE)0733-9429(2003)129:2(120)

Wilcock, P. R., Pitlick, J., & Cui, Y. (2009). *Sediment transport primer: Estimating bed-material transport in gravel-bed rivers* (RMRS-GTR-226; p. RMRS-GTR-226). U.S. Department of Agriculture, Forest Service, Rocky Mountain Research Station. https://doi.org/10.2737/RMRS-GTR-226

Williams, G. P. (1978). Bank-full discharge of rivers. *Water Resources Research*, *14*(6), 1141–1154. https://doi.org/10.1029/WR014i006p01141

Wohl, E. (2016). Spatial heterogeneity as a component of river geomorphic complexity. *Progress in Physical Geography: Earth and Environment*, *40*(4), 598–615. https://doi.org/10.1177/0309133316658615

Wohl, E., Bledsoe, B. P., Jacobson, R. B., Poff, N. L., Rathburn, S. L., Walters, D. M., & Wilcox, A. C. (2015). The Natural Sediment Regime in Rivers: Broadening the Foundation for Ecosystem Management. *BioScience*, *65*(4), 358–371. https://doi.org/10.1093/biosci/biv002

Wohl, E., & Cenderelli, D. A. (2000). Sediment deposition and transport patterns following a reservoir sediment release. *Water Resources Research*, *36*(1), 319–333. https://doi.org/10.1029/1999WR900272

Wohl, E., Marshall, A. E., Scamardo, J., White, D., & Morrison, R. R. (2022). Biogeomorphic influences on river corridor resilience to wildfire disturbances in a mountain stream of the Southern Rockies, USA. *Science of The Total Environment*, *820*, 153321. https://doi.org/10.1016/j.scitotenv.2022.153321

Wohl, E., Marshall, A. E., Triantafillou, S., Mobley, M., Means-Brous, M., & Morrison, R. R. (2024). Distribution of logjams in relation to lateral connectivity in the River Corridor. *Geomorphology*, *451*, 109100. https://doi.org/10.1016/j.geomorph.2024.109100

Wohl, E., & Scamardo, J. E. (2021). The resilience of logjams to floods. *Hydrological Processes*, *35*(1), e13970. https://doi.org/10.1002/hyp.13970

Wohl, E., & Scott, D. N. (2017). Wood and sediment storage and dynamics in river corridors. *Earth Surface Processes and Landforms*, *42*(1), 5–23. https://doi.org/10.1002/esp.3909

Wolf, E. C., Cooper, D. J., & Hobbs, N. T. (2007). HYDROLOGIC REGIME AND HERBIVORY STABILIZE AN ALTERNATIVE STATE IN YELLOWSTONE NATIONAL PARK. *Ecological Applications*, *17*(6), 1572–1587. https://doi.org/10.1890/06-2042.1

Wolman, M. G., & Miller, J. P. (1960). Magnitude and Frequency of Forces in Geomorphic Processes. *The Journal of Geology*, *68*(1), 54–74. https://doi.org/10.1086/626637

Woodget, A. S., Austrums, R., Maddock, I. P., & Habit, E. (2017). Drones and digital photogrammetry: From classifications to continuums for monitoring river habitat and hydromorphology. *WIREs Water*, *4*(4). https://doi.org/10.1002/wat2.1222

Workman, J. B., Cole, J. C., Shroba, R. R., Kellogg, K. S., & Premo, W. R. (2018). *Geologic map of the Fort Collins 30'×60' quadrangle, Larimer and Jackson Counties, Colorado, and Albany and Laramie Counties, Wyoming* (U.S. Geological Survey Scientific Investigations Map 3399, p. pamphlet 83 p., 1 sheet, scale 1:100,000). https://doi.org/10.3133/sim3399

Writer, J. H., Hohner, A., Oropeza, J., Schmidt, A., Cawley, K. M., & Rosario-Ortiz, F. L. (2014). Water treatment implications after the High Park Wildfire, Colorado. *Journal - American Water Works Association*, *106*(4), E189–E199. https://doi.org/10.5942/jawwa.2014.106.0055

Yarnell, S. M., Petts, G. E., Schmidt, J. C., Whipple, A. A., Beller, E. E., Dahm, C. N., Goodwin, P., & Viers, J. H. (2015). Functional Flows in Modified Riverscapes: Hydrographs, Habitats and Opportunities. *BioScience*, *65*(10), 963–972. https://doi.org/10.1093/biosci/biv102

Table 11. Site coordinates in NAD83 / UTM Zone 13N (meters)

	downstream		upstream	
Site	**northing**	**easting**	**northing**	**easting**
Bliss	4506848	437380	4506875	437109
Pasquinels	4505484	440843	4505397	440642
Black Hollow	4505674	444618	4505684	444345
Fire Lane	4505562	447094	4505765	446925
Indian Meadows	4504689	456357	4504913	456172
Kelley Flats	4503877	459026	4504146	458934
Dutch George	4504859	461897	4504566	461965
Stove Prairie	4503752	466531	4503668	466328
Hewlett Gulch	4504171	473647	4504254	473387
Gateway	4505763	479606	4505866	479347
Lions Park	4496702	488173	4496961	488082
T03 (Shields)	4494769	491812	4494933	491539
T04	4494215	492907	4494403	492725
T06	4492778	494474	4492919	494259
T08	4492023	496650	4491950	496384
T11	4489849	498317	4489956	498136
T11	4489773	498677	4489686	498497
T12 (Archery Range)	4488461	499929	4488732	499806

Table 12. Differences between measured RTK points and SfM DEM used in hydraulic modelling.

	RTK - DEM Elevation (m)			
Site	**Mean**	**Median**	**Slope**	**R^2**
Shields Street	-0.068	-0.058	0.848	0.944
Archery Range	0.032	0.01	0.76	0.884

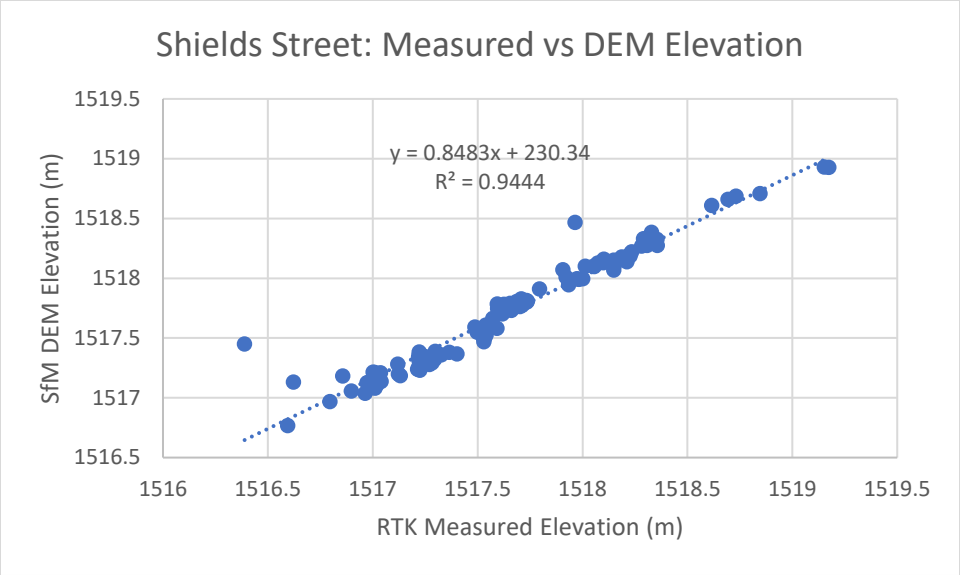

Figure 25. Plot of measured RTK points and SfM DEM at Shields Street.

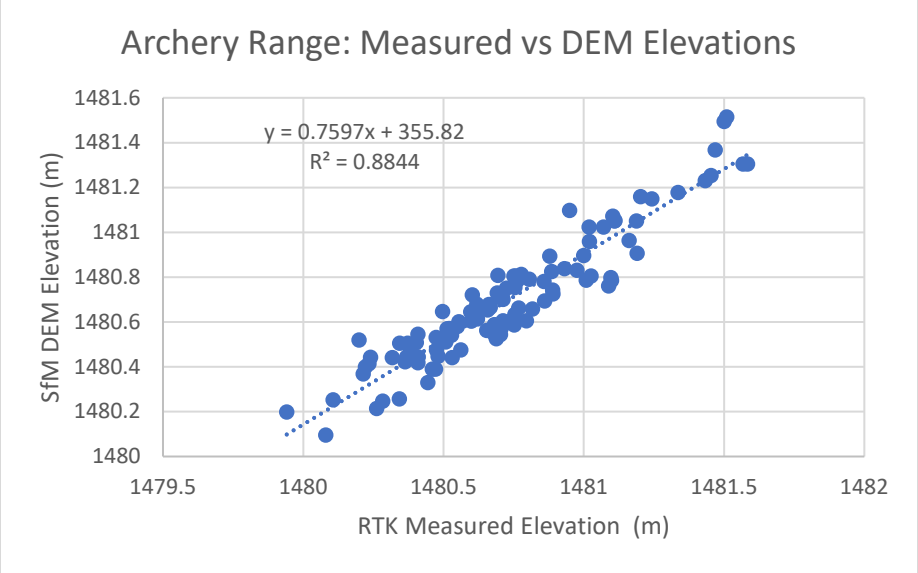

Figure 26. Plot of measured RTK points and SfM DEM at Archery Range.

Table 13. Interpretation of dimensionless shear stress values in terms of states of fine sediment flushing and coarse substrate mobilization. From Shanahan et al., 2014.

	Dimensionless shear stress (τ_*) referenced to d_{50}	
Sediment movement state	**Lower bound**	**Upper bound**
Fines and sand are stored		0.009
Fines and sand in motion	0.009	0.021
Surface cleaning and removal of fines	0.021	0.035
Initial movement of armor and substrate cleaning	0.035	0.06
General movement of and cleaning of substrate	0.06–0.084	–

Source: Adapted from Milhous, 2000, 2003.